Cleaner Chemical Engineering 8 (2023) 100115

Contents lists available at ScienceDirect

Cleaner Chemical Engineering

journal homepage: www.elsevier.com/locate/clce

Recent advances, challenges, and prospects of electrochemical water-splitting technologies for net-zero transition

Hasan Ozcan [a,b], Rami S. El-Emam [c,d], Selahattin Celik [a], Bahman Amini Horri [b,*]

[a] Department of Mechanical Engineering, Ankara Yildirim Beyazit University, Ankara, 06010, Turkey
[b] School of Chemistry and Chemical Engineering, University of Surrey, GU2 7XH, United Kingdom
[c] Faculty of Engineering and Applied Science, Ontario Tech University, Oshawa, ON, LG1 0C5, Canada
[d] Faculty of Engineering, Mansoura University, Mansoura, Egypt

ARTICLE INFO

Keywords:
Green hydrogen
Water splitting
Electrochemical technologies
Water electrolysis
LCOH
Net-Zero

ABSTRACT

This review paper presents state-of-the-art electrolytic-based hydrogen production technologies capable of helping to achieve the "net-zero" targets. It covers the recent advances in electrochemical water-splitting technologies, considering their maturity, durability, and operational aspects related to their near-term deployment. This paper aims to critically assess electrochemical technologies compatible with renewables, nuclear, or other clean energy sources with a high potential to be applied for green hydrogen production at scale. It also discusses the techno-economic aspects as well as the technological readiness of the potential carbon-free hydrogen production routes based on electrochemical approaches. With a comprehensive survey of the recent literature and extensive insight into current developments, the issues associated with deploying the electrolytic water splitting technologies are discussed, along with a review of their market readiness level to play a potential role in the transition journey from fossil fuel-based-economy into hydrogen-driven energy infrastructure. In addition, the paper provides insight into the legal strategies and the governmental incentives required to reach the so-called "net-zero" emission plans globally to enable green hydrogen for deep decarbonization of the industrial, transportation, and residential sectors. Near-term projects to deploy large-scale clean hydrogen production announced globally are also listed with their expected contribution toward the zero-emission targets. The result of this review shows that wind and solar photovoltaic energies, as the two most preferred renewable sources, can be used to drive Proton Exchange Membrane (PEM) and Alkaline Electrolysers (AE) at a cost range of USD 2 - 3 /kg of H_2. This figure is expected to decrease by more than 40 % until 2030 if these electrolyzers can be deployed at a large scale.

Introduction

Hydrogen is experiencing increasing momentum worldwide as an energy carrier and a clean fuel enabling us to achieve the "net-zero" emissions targets. The interest in hydrogen came in several waves in the past, driven by oil price peaks, supply-demand fluctuations, and tightening environmental protection policies. This, along with the significant engineering and scientific advances in the last few years, has caused a significant push towards deploying many demonstration plant activities on all related subjects to hydrogen production (e.g., production, storage, transportation, etc.). The current hydrogen-deployment wave comes from shifting towards industrializing clean hydrogen technologies to combat climate change following the growing number of local governments undertaking the relevant legislation to gain "net-zero" emission plans globally. The current deployment wave has significantly encouraged transformational changes to achieve the hydrogen economy and could finally lead to reaching the clean energy economy worldwide. The "hydrogen economy" is not new and has existed for decades. However, it has been mainly driven by fossil-based technologies so far. A significant portion of hydrogen demand globally (over 90 %) is currently used to produce (anhydrous) ammonia, a strategic product directly related to the fertilizer industry, and other chemicals like methanol, polymers, and refinery hydrogenation applications.

The fossil-fuel-based energy systems still dominate the global demand for power in the industrial, transportation, and household sectors. However, the share of renewables has slightly increased over the last 20

* Corresponding author.
E-mail address: b.aminihorri@surrey.ac.uk (B. Amini Horri).

https://doi.org/10.1016/j.clce.2023.100115
Received 24 April 2023; Received in revised form 28 August 2023; Accepted 11 October 2023
Available online 13 October 2023
2772-7823/© 2023 The Author(s). Published by Elsevier Ltd. This is an open access article under the CC BY license (http://creativecommons.org/licenses/by/4.0/).

years due to more attention to global warming issues with policymakers (Newell and Raimi, 2020). Electrification of the transport sector seems possible in the near- to mid-term to combat global warming-related issues while fueling industry and residents are energy-intensive and costly to be compensated by renewable electricity (Hausfather and Peters, 2020). Hydrogen, as a clean fuel produced from water splitting and electrified by renewable sources, is considered 'green' and a sustainable alternative to fossil fuels for future plans to decrease emissions (van Renssen, 2020). The utilization of hydrogen for major sectors has drawn significant interest after the bold decision made by the *European Union* to reduce emissions by up to 90 % by 2050 to become the first emission-free continent in the world (Silander, 2020). In order to accomplish this ambitious plan, there have been proposals such as the concept of "blue" hydrogen production, which, in principle, is deployed by integrating a Carbon Capture and Storage (CCS) unit into the conventional steam-methane reforming (SMR) processes. This resolution has not been commonly approved by the energy research and manufacturing community due to the dependence of the technique to fossil fuels, the potential risks of the process (e.g., uncontrolled/accidental methane leakage into the atmosphere) and low efficiency of the current CCS units (Newborough and Cooley, 2020). In addition, several strategies are on board to decrease methane-related emissions, which could potentially contribute to more than half of world emissions in the next 20 years; therefore, the use of CCS-SMR technologies for producing 'grey' and 'blue' hydrogen might not arguably meet the targets to neutralize the environmental CO_2 emissions in the first half of the century (Peters et al., 2020). The other clean energy supply approach is the so-called "turquoise hydrogen", which uses fossil fuels by separating carbon in the form of a solid residue (non-gaseous carbon dioxide emission) through certain techniques (Newborough and Cooley, 2020). Hydrogen can also be mixed with natural gas pipelines for grid applications (industry, residential, transportation, etc.). This approach can contribute to decreasing CO_2 emissions by 6.5 % if "green" hydrogen is used. The term "green" hydrogen denotes a water-splitting process supplied with renewable (or nuclear power) as a resource of energy (Ishaq and Dincer, 2020). The green hydrogen production approach is the most promising pathway for deeply decarbonizing the environment and achieving global "net-zero" emission targets.

"Clean hydrogen" is a generic term used to describe the technical pathways applied for producing carbon-free hydrogen. This includes the use of renewable energy sources to drive the hydrogen production plant (i.e., green hydrogen) and nuclear-driven hydrogen production (i.e., purple hydrogen). Any involvement of fossil fuel is not considered even if carbon capture is employed (i.e., grey, blue, or turquoise). Over the past two years, several countries around the world launched national programs to implement clean hydrogen technologies (with a focus on renewable-driven hydrogen) in their strategic energy plans and as part of their post-COVID recovery packages. Today, there are only 39 countries that have already legislated supporting policies and legal strategies for hydrogen production and application through the "net-zero" emission plan. However, implementing such comprehensive programs to enable energy transition towards zero/net-zero emissions would be associated with several barriers. This energy transformation prospect would need a global revolutionary change in many directions, such as developing the infrastructure required to deploy low-cost carbon-free hydrogen, legislating supporting policies, improving public awareness, and financing the industrial, transportation, and residential projects to adapt to hydrogen.

The use of hydrogen as an alternative fuel and energy carrier has a long history of debates for possible use, starting with the oil crisis at the beginning of the 1970s (El-Emam et al., 2023; Gabriel et al., 2022). Even though a fast induction of initial ideas for hydrogen production has been present, no further research has been conducted in the first couple of decades. However, the amount of research significantly increased when concerns about global warming, increasing population, and limited fossil resources came to the public's attention in the late 1990s (El-Emam and Özcan, 2019). Hydrogen is presently used in industries such as fertilizer production, gas purification, replacement to fuel gases in iron making, welding, and chemical feedstock synthesis (Hu et al., 2020; Pivovar, 2017). Hydrogen is still primarily produced with conventional fossil-fuel-based methods, where renewable hydrogen corresponds to only about 4 % of the total production figure globally.

Furthermore, 15 % of the globally produced renewable hydrogen comes from facilities where green hydrogen production is not the primary purpose – such as the chloralkali process using alkaline electrolyzers where chlorine gas is the main product (Birol, 2019a). The total hydrogen demand in the world is recently reported as nearly 70 Mt, while it is predicted that hydrogen may supply up to 20 % of global energy demand within the next three decades (Safari and Dincer, 2020; Council, 2017). It is thus essential to induct clean, more efficient, technically, and economically feasible hydrogen production systems to the market to provide this expected significant demand in the upcoming decades. However, the penetration rate of green hydrogen technologies into the available market is still slow.

Since most hydrogen globally produced today (above 96 %) comes from fossil fuels associated with significant CO_2 emissions, the current hydrogen market needs profound decarbonization to meet the "clean hydrogen" requirements. Natural gas is the primary fossil fuel for producing hydrogen, accounting for almost half of all hydrogen generation globally, followed by off-gases and coal (Muradov, 2017). Even though the SMR process is considered the standard platform for producing hydrogen at scale, it is associated with emitting about 10.4 kg eq. CO_2/kg H_2. In the case of heavy oil, this figure is even poorer through various gasification processes required, with a dramatic value approaching about 24 kg eq. CO_2/kg H_2 (McDowall and Eames, 2006). Water electrolysis can also be associated with a high eq. CO_2/H_2 ratio, if its power is supplied from the grid based on the fossil-fuel power plants.

In the last couple of decades, the cost of green hydrogen production decreased with increased technology maturity. However, it is still not competitive with the price of grey hydrogen produced from fossil fuels. This mainly depends on the price list in the oil & gas market that follows the supply-demand model and, therefore, is subject to change in the future. In addition, the carbon tax is being considered by policymakers as an incentive tool, which could add a high cost to the grey hydrogen market in the next few years (Muradov and Veziroğlu, 2005). The carbon tax figure applied by the local governments varies from $0 to $100 per ton of eq. CO_2 according to the production plants' location, emission severity, and national/international regulations (Marron et al., 2015). In the worst-case scenario, the cost of hydrogen from natural gas might increase by about 15 % when the carbon tax is applied at the mid-range level globally. All these concerns bring together a mindset to move towards emission-free hydrogen technologies as soon as possible to address the tightening environmental protection guidelines and the net-zero emission targets.

Green hydrogen, in principle, is defined as the utilization of renewables to power the water-splitting process, with producing oxygen as the only by-product. Electrolysis is one of the most common techniques applied for water splitting; however, it only stands for about 4 % of the global hydrogen production market. The electric power required for the existing electrolysis technologies is as high as about 4.9 kWh/Nm^3 H_2, mainly due to high overpotentials through electrolysis cells. If the water-electrolysis power is supplied from conventional fossil fuels, the equivalent carbon emissions of the overall process could correspond to about 28 kg eq. CO_2/kg H_2, which is even higher than coal-based hydrogen generation. Therefore, the only approach to minimize the carbon emission associated with water electrolysis is to supply its electric power from renewables (Muradov, 2017; Muradov and Veziroğlu, 2005; Council, 2004). Water electrolysis, in principle, does not require any additional heat; however, the electrolysis cell efficacy would be maximized if the electrolyte solutions and/or water feeds-stream were heated to reach certain temperatures (above 60 °C, depending on the type of technology) (Carmo et al., 2013). Proton exchange membrane (PEM),

anion exchange membrane (AEM), and alkaline electrolysis (AE) processes are the three standard platforms for water electrolysis operating at a low temperature (below 100 °C) with a theoretical potential of about 1.25 V. Comparably, high-temperature steam electrolysis (HTSE) require a lower theoretical voltage (0.99 V) by compensating for the rest of the energy requirement from the superheated steam supplied at a high temperature (above 800 °C). The HTSE process can only be a "zero-carbon emission" when this excess heat for steam generation is supplied from renewable sources such as concentrated solar panels, next-generation nuclear reactors, or the excess heat from industries supplied by renewable electric power. Therefore, the development of a centralized production plant with the integration of hybrid resources (renewable heat and power) is essential to deploy hydrogen with low-carbon emission (Laguna-Bercero, 2012), (Al-Qahtani et al., 2021).

Scope and objectives

This paper aims to provide an up-to-date status of the electrolytic-based hydrogen production technologies with an appropriate analysis of the existing clean hydrogen facilities installed globally to approximate the cost of green hydrogen production in the current market. With a critical literature review approach, this study focuses mainly on the comparative environmental assessment of clean hydrogen production in a broader view. Throughout the paper, the term "clean hydrogen" refers to carbon-free and low-carbon hydrogen through renewables, nuclear electricity, and/or thermal energy harvested thereof. Electrochemical hydrogen production technologies that are compatible with carbon-free energy sources and with the potential for large-scale hydrogen production are discussed. Advances in electrochemical water-splitting R&D are presented, including the use of new materials and catalysts and recent progress in overcoming durability issues of novel methods. Since this review considers screening the electrochemical technologies that have already been introduced to the market, the other water-splitting techniques with a low technology readiness level (TRL), such as solar-light-based water-splitting, including photoelectrochemical technologies and radiochemical methods, are excluded from the analysis in this work (Acar et al., 2019; Fujishima and Honda, 1972). Biological hydrogen generation would also be excluded through the screening due to its potential for emissions with no CCS scenarios integrated. The feasibility of the available technologies or near-term deployment possibilities is surveyed and discussed. This covers the technoeconomic and extended to discuss the market penetration and readiness of clean hydrogen production and other relevant social and environmental aspects.

Electrochemical technologies: status and advances

Three main electrolytic water splitting methods are classified into four major categories, including AE, PEM, HTSE, and AEM methods. PEM and AE operate at ambient conditions or slightly higher temperatures, while HTSE needs elevated temperatures. Anion exchange membrane (AEM) water electrolysis is also a recent alternative to the AE technique, combining the advantages of applying a polymer-based membrane like PEM electrolyzers for the alkaline environment.

PEM water electrolysis

Low operating pressures, current density limitations, and problems associated with diaphragm use in conventional alkaline electrolyzers led researchers to find a certain solution with solid polymer electrolytes, later referred to as polymer electrolyte membrane (Nafion®) or proton exchange membrane water electrolysis (Carmo et al., 2013; Russell et al., 1973). PEM electrolyzers are known for advantages such as high operating pressures and current densities, high gas purity, compact design, and high efficiency in providing a cost-effective solution (Slade et al., 2002). Pressures higher than 100 bars are achievable only if the cathode part is pressurized to prevent challenges of high-pressure oxygen presence (Bolobov, 2002). The corrosive nature of the membrane requires operation at low pH values and high voltages that require expensive noble materials such as platinum and titanium, possibly making the capital costs higher. Comprehensive reviews on electrocatalysis for oxygen evolution and hydrogen evolution reactions (OER and HER), current collectors, membranes, and separators, as well as modeling works, have been previously conducted (Carmo et al., 2013; Kumar and Himabindu, 2019). Recent advances in modeling aspects and materials are also reviewed here. Another detailed survey is conducted for solid acids as electrolytes for PEM (Goñi-Urtiaga et al., 2012). Bipolar plates mainly form PEMs, gas diffusion layers, and membrane electrode assemblies with some other supporting layers. For a durable operation, material characteristics, reactivity through and between layers, cell assembly configurations and feed water purity are of importance.

Conventional PEMs utilize platinum at HER and iridium oxide at OER, being highly noble, making it costly. Some efforts are undertaken to replace noble metals using carbon-supported catalysts, cobalt clathrochelates at the HER, and manganese-based substances to replace iridium at the OER (Millet et al., 2011; Pantani et al., 2006; Medhoui et al., 2006). Desired OER performances have been obtained using nanocrystalline electrocatalysts based on iridium oxide with ruthenium oxide and/or tin oxide additions or when mixed with tantalum pentoxide (Tunold et al., 2010). Antimony oxide has also been considered as a support structure to iridium oxide (Saveleva et al., 2020). Reactive magnetron sputtering has been used to deposit iridium oxide to be used as an efficient catalyst in PEM electrolysers, showing the method to be a promising alternative for catalysis deposition methods (Slavcheva et al., 2007). Adams fusion method is used to synthesize iridium-based electrocatalysts where Ru introduction enhanced the PEM electrical formation while Sn introduction severely depreciated the operation (Mayousse et al., 2011). Hydrothermal formation of Molybdenum disulfide (MoS_2) is accomplished, and trials indicated that MoS_2-coated PEM showed good electrocatalytic activity with no degradation at 200 h operation (Kumar et al., 2016). Protective coatings for bipolar plates and current collectors in PEM electrolyzers using vacuum plasma spraying is another method to prepare corrosion-resistant plates for low degradation (Lettenmeier et al., 2017).

Molybdenum disulfide (MoS_2) and carbon black (Vulcan®) have been considered promising replacement species for precious metals, with experimental validations showing that their use could be an inexpensive and efficient alternative (Corrales-Sánchez et al., 2014). Au and TIN-based coatings are considered to replace titanium-based coating in bipolar plates of PEM for possible cost-effective solutions for the operation where possible ways to control the changes in pH value are reported to prevent failures in the long-term operations (Langemann et al., 2015). Several coatings are proposed for stainless steel bipolar plates in PEM, including Ti and Pt/Ti mixtures, to show the possibility of using spray-coated stainless steel (Gago et al., 2016). Some selected materials are used as alternatives to titanium-based bipolar plates where tantalum and niobium showed similar features to those of titanium under operation (Lædre et al., 2017). Even though PEM technology is matured with industrial applications, further research for material interactions in the cell and methods for manufacturing catalysts and support materials are underway for extended cell life and more feasible operation (Ayers, 2021; Böhm et al., 2021). Fig. 1 represents a detailed scheme of PEM electrolyzers with potential materials being used for electrocatalysis, diffusion layers, and coating.

Mechanical degradation (reduced porosity of diffusion layers and mass transport limitations due to clamping pressures), chemical degradation (poisoning by foreign ions, feed water impurities), thermal degradation of membranes, hydrogen embrittlement, corrosion and passivation of bipolar plates, and deactivation of catalyst due to agglomeration and dissolution are main issues that affect the durability of PEM electrolyzers (Liu, 2021). The membrane electrode assembly (MEA) fabrication procedure is crucial for the mechanical stability of the cell. An optimum hot pressing procedure may significantly increase

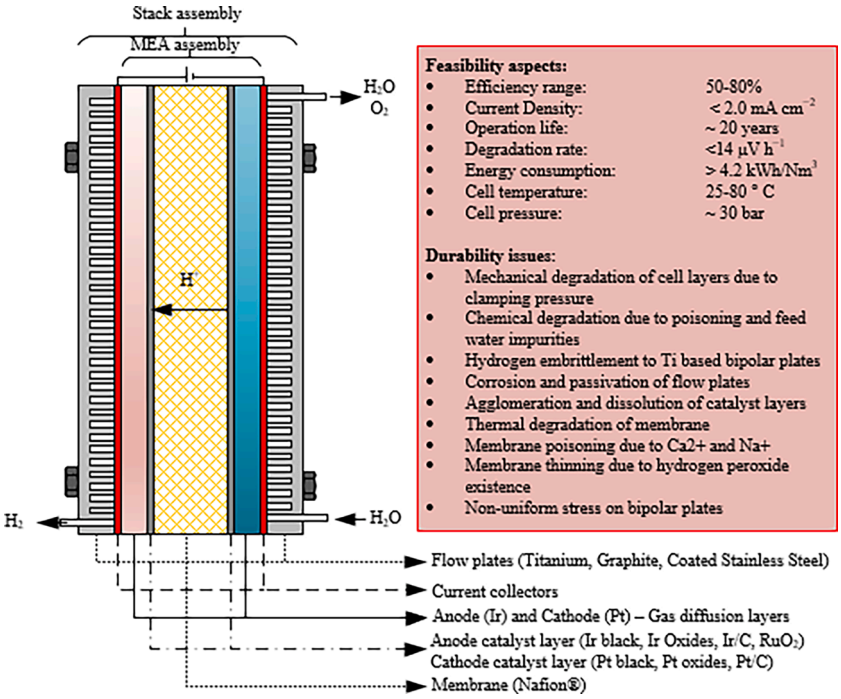


Fig. 1. Working principle, durability, and feasibility aspects of PEM electrolyzers.

stable operation (Siracusano et al., 2018a). Dissolution of electrocatalysts causes fast degradation of electrochemical surface area and mass activity above 1.8 V (Oh et al., 2016). Poisoning of the metallic cation is another common issue due to impurities such as sodium and calcium that significantly increase the charge transfer resistance and result in higher potentials (Wei et al., 2010). Agglomeration of catalyst particles results in the reduction of the active catalyst area that is available for the electrochemical reaction and cathode current density. This issue generally starts occurring when the cell is operated over 1000 h (Paciok et al., 2015; Terezo et al., 2001). An increased cell voltage is also required when surface oxidation between the support and the anode is present due to the prevention of electron flow (Khatib et al., 2019). Membrane failures are possible due to mechanical stresses around bipolar plates, non-uniform compression at the surface of current collectors, Ti presence on the membrane surface, the texture of the gas diffusion layer that causes holes on the membrane surface at high clamping pressure, gas crossover blockage at very high pressures, the insufficient or high flow rate of water, uneven distribution of water on the bipolar plate and membrane thinning due to formation of hydrogen peroxide on the electrode surface (Debe et al., 2012; Millet et al., 2012; Chandesris et al., 2015; Tang et al., 2007; LaConti and Swette, 2010).

Bipolar plates were initially made of graphite; however, its high cost, weak mechanical strength, challenges in fabrication, and low operational life urged an investigation of other materials such as titanium, aluminum, and stainless steel (Hung et al., 2005). The mechanical strength of titanium is lower than graphite, and hydrogen embrittlement is highly possible when the hydrogen solubility limit is exceeded. It is also reported that passivation of the titanium bipolar plates is present at high cell potentials (Briant et al., 2002; Tawfik et al., 2007). Stainless steel is, so far, the best replacement as it is low-cost, has no or low embrittlement and has easy machinability with problems related to corrosion at high potentials (Gago et al., 2016). Increased operational life, low-cost materials, and durable operation of bipolar plates are of crucial importance for the efficient operation of PEM electrolyzers since they account for almost half of the total PEM cell cost (Feng et al., 2017). Further research is still being conducted for durable operation by overcoming issues related to catalytic layers, flow plates, and MEAs to reduce the costs and issues causing degradation and to increase the operating pressure range.

PEM electrolyzers can show energy efficiencies between 50 and 80 % at higher operational pressures and energy densities than those of alkaline electrolyzers, while stack size and operational life are lower. Due to overpotentials, durability, and degradation issues, specific energy consumption ranges between 4.2 to 5.6 kWh/Nm^3 (Carmo et al., 2013). Mathematical and thermal models of PEM at the cell and stack level are widely available in the literature to model thermal and economic aspects. Early models are described, and some studies have been conducted to comparatively represent empirical models of PEM (Onda et al., 2002; Awasthi et al., 2011; García-Valverde et al., 2012; Falcão and Pinto, 2020). The performance of the electrolyzers alone may not provide an overall picture unless the balance of components and resource efficiencies are considered. Therefore, overall system studies are available in the recent literature reporting aspects of green hydrogen via PEM electrolysis. Solar electrolysis via PEM has potential problems such as intermittent operation, the output pressure of hydrogen, and the handling of generated oxygen as the by-product (Barbir, 2005). Table 1 shows the comparison of studies conducted in the literature for PEM water electrolysis with a broad perspective. Most of the studies were carried out at a temperature of 80 °C, and the results of the experiments at a maximum of 120 °C and at least room temperature (RT) are added to the table. Most of the PEM water electrolysis processes listed in Table 1 were performed at ambient pressure. In addition, some studies carried out tests in the pressure range of 3–25 bar (Grigor'ev et al., 2001; Ioroi et al., 2002; Antonucci et al., 2008; Baglio et al., 2009; Polonský et al., 2014; Skulimowska et al., 2014; Kokoh et al., 2014), as well as other studies that carried out tests above 50 bar (Russell et al., 1973; Grigoriev et al., 2009a; Millet et al., 2009; Millet et al., 2010).

Alkaline water electrolysis

Alkaline water electrolysis is well-known for being the first commercial method to split water. The technique was initially proposed in the 18th century and further developed in the 19th century, with hundreds of industrial-scale electrolyzers already available in the first decade of the 20th century (Zhang et al., 2011; Chisholm and Cronin, 2016). Even though PEM water electrolysis is proposed as an alternative

Table 1
Detailed comparison for PEM water electrolysis studied in the literature.

Membrane	Ionomer (C %N.A%)	Anode Catalyst	Cathode Catalyst	Anode loading mg/cm^2	Cathode loading mg/cm^2	Anode Current Collector	Cathode Current Collector	Cell Area (cm^2)	Number of Cells	E (Volt)/ Cell	Current Density (mA/ cm^2)	Cell Temperature (°C)	Operational Life Test (h)	Reference
Nafion	x	RuO2	Pt black	4	4	x	x	46.6	1	1.73	1072	52	6700	(Sedlak et al., 1981)
Nafion 125	x	Ir	Pt	6	6	Pt/Ti	Pt/Ti	50	1	1.59	500	90	x	(Takenaka et al., 1982)
Nafion 117	x	Pt	Pt	1	1	Porous Ti	Porous Ti	50	2	2.13	500	80	7000	(Millet et al., 1996)
Nafion 117	x	Pt/Ir	Pt	x	x	Ti fiber sintered plate (Pt Coated)	C	2500	10	1.74	1000	80	5000	(Kondoh et al., 2000)
MF4SK	x	Ir Black	Pt black	x	x	x	x	20	1	1.7	1000	120	x	(Grigor'ev et al., 2001)
Nafion 115	9 % Nafion	Pt/Ir Black (Johnson Matthey)	Pt/Ir Black (Johnson Matthey)	4	4	x	x	10	1	1.8	500	80	x	(Ioroi et al., 2002)
Nafion	20 %N.	IrO2	10–40 % wt. %Pt on Carbon (Johnson Matthey)	2	0.4	Sintered Porous Titanium	Sintered Porous Titanium	5	1	1.65	1000	80	x	(Rasten et al., 2003)
Nafion	N.5 %	RuO2	40 %Pt/C	10	0.4	Ti	Ti	9	1	1.88	1100	RT	x	(Ma et al., 2006)
Nafion 115	5 %N.10 %	IrO2 40 %Sn/Ir 80 %Sn/Ir	20 % Pt/ Vulcan XC-72 R (E-TEK)	2	0.4	Sintered Porous Titanium	Sintered Porous Titanium	x	x	1,65 1,70 1,81	1000	80	x	(Marshall et al., 2006)
Nafion 115	5 %N.10 %	Ir0.6Ru0.2Ta0.2O2 Ir0.6Ru0.4O2	20 % Pt/ Vulcan XC-72 R (E-TEK)	2	0.4	Sintered Porous Titanium	Sintered Porous Titanium	x	x	1,60 1,57	1000	80	x	(Marshall et al., 2007)
Nafion 115	N.5 %	Pt/IrO2	30 %Pt/C	3	0.5	Ti mesh	C Toray	5	1	1.8	1000	80	10	(Shidong et al., 2007)
Nafion 115	30 %N.5 %	IrO2	Pt black	2	2.25	Au/C Paper	C Toray	5	1	1.66	1000	80	x	(Zongqiang et al., 2007)
Nafion 115	10 %N.	Ir Black	30 %Pt/C/ Vulcan XC-72 30 %Pd/C/ Vulcan XC-72	2.4	0.7	Sintered Porous Titanium	Sintered Porous Titanium	7	1	1,66 1,70	1000	90	100	(Grigoriev et al., 2008)
Nafion 112	N.5 %	Ir Black Ru IrO2A IrO2C RuO2 Ir0.5Ru0.5O2	30 %Pt/C (T.K.K. Corp.)	3	0.5	C Toray	C Toray	5	1	1,72 1,80 1,63 1,62 1,65 1,65	1000	80	x	(Shidong et al., 2008)
Nafion 115 Nafion-SiO2	N.5 %	IrO2	30 %Pt/C	5	0.8	Sintered Porous Titanium	Sintered Porous Titanium	5	1	1.9	2100	120	300	(Antonucci et al., 2008)
Nafion 1035	25 %N.	IrxRu1−xO2	30 %Pt/C	1.5	0.5	C Toray	C Toray	5	1	1.622	1000	80	x	(Cheng et al., 2009a)
Nafion 117	x	Ir Black	Pt black	2	0.8	Pt/ Sintered Porous Titanium	Pt/ Sintered Porous Titanium	50	1	1.71	1500	90	x	(Grigoriev et al., 2009a)
Nafion 115	15 %N.5 %	Ir Black	Pt black	2	0.8	Sintered Porous Titanium	Sintered Porous Titanium	7	1	1.67	1000	90	x	(Grigoriev et al., 2009b)

(*continued on next page*)

Table 1 (*continued*)

Membrane	Ionomer (C %N.A%)	Anode Catalyst	Cathode Catalyst	Anode loading mg/cm^2	Cathode loading mg/cm^2	Anode Current Collector	Cathode Current Collector	Cell Area (cm^2)	Number of Cells	E (Volt)/ Cell	Current Density (mA/ cm^2)	Cell Temperature (°C)	Operational Life Test (h)	Reference
Nafion 115	x	Ir Black	Pt/C	2.4	x	x	x	250	12	1.88	1000	50	20,000	(Millet et al., 2009)
Nafion 1035	25 %N.5 %	Ir0,4Ru0,6O2	30 %Pt/C (T.K.K. Corp.)	1.5	0.5	C Toray	C Toray	5	1	1.65	x	80	x	(Cheng et al., 2009b)
N. TiO_2	33 %N.5 %	IrO2	30 %Pt/C (T.K.K. Corp.)	5	0.8	Ti Mesh	ELAT	x	x	1.9	1800	80	x	(Baglio et al., 2009)
Nafion 115	15 %N.5 %	Ir Black	20 %Pd/C (XC72)	2	0.35	Sintered Porous Titanium	Sintered Porous Titanium	250	4	1.72	1000	85	x	(Millet et al., 2010)
N.	N.5 %	Ir Black	20 %Pt/C (Johnson Matthey)	5	1.5	x	x	4	1	2	1600	x	x	(Guoqiang et al., 2010)
Nafion 115	33 %N.	IrO2	30 %Pt/C (E-TEK)	2.5	0.5	Ti Mesh	ELAT	100	9	1.6	600	70	x	(Siracusano et al., 2012)
SPSF	33 %N.	IrO2	Pt/C	2.5	0.4	Ti Mesh	ELAT	5	1	1.8	1100	80	x	(Schalenbach et al., 2013)
Nafion 115	x	IrO2	Pt/C	2.5	0.5	Ti Mesh	ELAT	100	9	1.65	600	70	x	(Di Blasi et al., 2013)
Nafion 115	15 %N.	IrO2:10 wt.% F	Pt black	x	x	Ti Mesh	C Paper	5	1	2	1100	40	x	(Kadakia et al., 2014)
Nafion 115	x	Ir/Pt	Pt	2.5	2.5	Porous Titanium	Porous Titanium	7	1	2.3	1000	90	5500	(Grigoriev et al., 2014)
Nafion 117	x	IrO2/TaC	Pt/C	x	0.5	ELAT	ELAT	4	1	1.7	940	130	x	(Polonský et al., 2014)
PTFE-reinforced Nafion	x	IrO2	Pt/C	1.5	0.5	x	x	100	6	1.9	1000	80	x	(Rozain and Millet, 2014)
Nafion 117	x	IrO2	MoS2/XC72 MoS2/RGO	2	5	Porous Titanium	Porous Titanium	4	1	1.9	300	80	18	(Corrales-Sánchez et al., 2014)
Nafion 212	5wt% Cs1.5HPA	IrO2/Sb-SnO2	Pt/C	1.5	0.5	Carbon cloths/ Gold Plated Ti	Carbon cloths/ Gold Plated Ti	1	1	1.59	2000	80	570	(Liu et al., 2014)
Aquivion E87–12S	33 %N.	IrO2	Pt	2	2	Ti	MPL	6.25	1	2	2000	120	x	(Skulimowska et al., 2014)
Nafion 115	5 %N.5 %	Ir Black	Pt/C (Johnson Matthey)	1.5	0.4	Porous Titanium	Carbon/ Pt Coated Ti Mesh	160	9	1.68	1000	60	7800	(Sun et al., 2014)
Nafion 115/117	27 %N.10 %	Ru/Ir/Sn/O2 Ru/Ir/Ti/O2 Ru/Ir/O2	Pt/C (Tanaka)	x	2.5	Sintered Porous Titanium	C (SGL 34BC)	5	1	1.88	1000	60	400	(Kokoh et al., 2014)
Aquivion E87–12S	33 % Aquivion	IrO2	Pt/C	2	0.3	Ti	x	5	1	1.8	3200	90	x	(Siracusano et al., 2014)
Nafion 117		Ir/Ebonex	Pt/C (E-TEK)	0.2	0.2	(TPHG-30, E-TEK)	(TPHG-30, E-TEK)	x	x	x	x	x	x	(Slavcheva et al., 2015)
Aquivion E87–12S	33 % Aquivion20 %	Ir0.7Ru0.3Ox	Pt/C	1.5	0.4	Ti Mesh	Ti Mesh	5	1	1.9	4000	90	x	(Siracusano et al., 2015)
Nafion 117	x	IrO2	Pt	0.8	0.5	HT ELAT	HT ELAT	4	1	1.5	1200	150	x	(Mališ et al., 2016)

(*continued on next page*)

Table 1 (*continued*)

Membrane	Ionomer (C %N.A%)	Anode Catalyst	Cathode Catalyst	Anode loading mg/cm^2	Cathode loading mg/cm^2	Anode Current Collector	Cathode Current Collector	Cell Area (cm^2)	Number of Cells	E (Volt)/ Cell	Current Density (mA/ cm^2)	Cell Temperature (°C)	Operational Life Test (h)	Reference
Aquivion	33 % Aquivion20 %	Ir Black IrO2	Pt (Vulcan XC72)	0.4	0.1	Pt-coated titanium fiber mesh	GDL ELAT	5	1	1,9 1,65	1000	80	1000	(Siracusano et al., 2017)
Aquivion E098–09	25 % Aquivion	IrRuOx	Pt Black	3	3	x	x	x	x	1.7	1000	55	5700	(Siracusano et al., 201b)
Nafion 115	x	IrO2	Pt/C (Tanaka)	2.3	1	Sintered Porous Titanium	SGL Sigracet 28BCE carbon sheet	25	1	x	2000	80	500	(Frensch et al., 2019)
Nafion 115	x	RuO2	Pd/B3-CNPs	3	0.7	Porous Titanium	Porous Titanium	25	1	2.04	1000	80	x	(Shiva Kumar and Himabindu, 2020)
Nafion 115	x	IrO2 (Tanaka)	NiMo (graphene-encapsulated)	1	5	Porous Titanium	Porous Titanium	4	1	1.67	1000	80	100	(Tajuddin et al., 2021)
Nafion 115	x	IrO2/TiO2	Pt Black	3	3	Porous Titanium	Porous Titanium	25	1	1.9	2000	80	100	(Doan et al., 2022)

to this method, AE is still largely available with being a mature process, its applicability at large scale, high operational life, high purity products, and low degradation characteristics. With novelties in metal oxide-based electrolysers with alkaline electrolytes AEs may show competitive efficiencies (Schalenbach et al., 2016; Horri et al., 2019). The main components of the AE are the electrodes, a liquid electrolyte mainly with a KOH and NaOH solution, and a membrane to separate electrodes that lets OH^- ions transfer. The porous diaphragm is generally made of Zirfon, where the alkaline solution transfers trough while H_2 and O_2 mixing is prevented. As the most active non-noble metal, nickel-based materials are utilized as electrodes in AE, while stainless steel is also considered for its better catalytic activity at high temperatures during the OER (Cherevko et al., 2016; Schalenbach et al., 2018). The operational pressure of this method is around 30 bars with efficiencies up to 70 % at low operating temperature ranges (30–70 °C). The specific energy consumption at the stack level is also competitive to those of PEM electrolysis at a range of 4.2 – 5.9 kWh/Nm^3 H_2, while the degradation rate is well below PEM at a rate of <3 μV/h (Carmo et al., 2013). Even though the AE technology is a proven and widely used method, there is a large interest in further research to enhance operational characteristics of the AE, and advances are on the way (David et al., 2019; Santos et al., 2021).

Operating AE at high pressures has previously been claimed to be highly efficient since the product gas does not need further compression for transportation (Onda et al., 2002; Ziems et al., 2012). However, issues such as operational complexity, hydrogen embrittlement, corrosion, and high-pressure resistance material selection make the operation more costly and less efficient (Roy et al., 2006). Pressures above the upper limit of AE at high temperatures have also been studied, and it is reported that it is possible to produce high-purity hydrogen at high efficiencies at an economically feasible level (Ganley, 2009). There have not been an adequate number of studies to validate that high-temperature operation does not deter the electrode and membrane material properties (Allebrod et al., 2013).

Hydrogen formation at the cathode is significantly influenced by the electrolyte concentration, temperature, electrode type, and properties (Zeng and Zhang, 2010). The surface roughness and structure of the electrode are effective at HER. Ni, Pb, Au, Fe, Zn, Co, and Pt electrodes are used at the cathode electrode showing similar hydrogen production rates (Bockris et al., 1980; Lee, 1971). The anode electrode is mainly made of and/or coated with Ni, Pt, Ir, Co, Rh, and Fe metals, while Fe and Co represent higher reaction rates at the anode (Miles et al., 1978). Ni, La, and Co-based oxides are utilized as electrocatalysts for the cathode electrode, while Ni-based oxides and their mixtures with Ti, Al, Zn, and Co are used for electrocatalysts for the anode electrode (Singh et al., 2007; Wendt et al., 1989; Raj, 1993). Most of the available studies for electrocatalysts for electrode materials were conducted decades ago, and further studies are required primarily to overcome operational limitations in the AE technology (Sapountzi et al., 2017).

Reaction rates at HER and OER are not only affected by the electrocatalysts but also by the electrolyte recirculation and bubble formation. A higher amount of product generation results in increased amounts of bubbles in the cell compartments and should be removed rapidly before forming a layer between the electrode and electrolyte, resulting in a decreased production rate. Therefore, optimal recirculation of the electrolyte is essential, and the geometry of the electrode might also prevent this common issue (Zhang and Zeng, 2012; Mandin et al., 2014). A recent work utilizing PTFE (polytetrafluoroethylene) Gortex gas diffusion layers resulted in overpotentials significantly decreasing primarily at the anode compartment of AE (Tiwari et al., 2019). Other aspects, such as the electrolyzer configuration being bipolar and monopolar, inlet feed water purity, electrolyte conduction rate, current density limitations due to fast bubble formation, electrode material stability, and distance between electrodes, have been comprehensively discussed elsewhere (Zeng and Zhang, 2010). The presence of CO_2 in the air also jeopardizes the electrolyte by forming

Potassium Carbonate, resulting in decreased ionic conductivity of the KOH electrolyte. Therefore, proper sealing is crucial to prevent the electrolyte from forming unwanted structures (Naughton et al., 2011). A schematic of a common AE system is represented in Fig. 2.

Table 2 compares studies conducted in the literature for alkaline water electrolysis. Most of the studies were carried out in the temperature range of 50 °C to 80 °C and at ambient pressure. It has also been presented in studies investigating the effect of the pressure of 40 bar and above (Allebrod et al., 2014; Kuleshov et al., 2019). It has been observed that alkaline electrolysis efficiency varies between 60 % and 80 %, and the energy consumption range is between 3.35 and 5.6 kWh/Nm^3. In addition, it has been reported that there is a degradation in the range of 5 to 480 μV/h, in the electrolyser cells, mostly due to electrode deterioration (Kuleshov et al., 2019; Kim et al., 2015; Egelund et al., 2016; Sivanantham and Shanmugam, 2017).

Anion exchange membrane water electrolysis

AEM electrolysis is a new method of water electrolysis that was recently proposed, and its working principle reflects a combination of PEM and AE electrolysis (Leng et al., 2012). AEM electrolyzers are considered as better performing alternatives to other methods to reduce the costs of the electrolyzer by phasing out the use of noble electrocatalysts and other issues related to AE and PEM electrolyzers (Henkensmeier et al., 2021; Miller et al., 2020a). Electrodes are separated by a thin polymer membrane like the PEM electrolyzers; however, hydroxide ions transfer charges as in AE, resulting in high pH in the system that reduces issues related to an acidic environment that leads to corrosion which is one of the major problems that affects the durability of both AE and PEM (Vincent and Bessarabov, 2018). A schematic of the AEM electrolyzer is represented in Fig. 3.

The AEM electrolyzer operational condition is vital to claim its superiority over other well-known technologies. Higher current densities above 500 mA/cm^2 accelerate the hydrogen generation, resulting in intensive bubble formation in the electrolyte and resulting in increased overpotentials; therefore, optimal hydrogen generation and electrical efficiency conditions should be taken into account (Zoulias et al., 2004). AEMs work at a temperature range of 50–80 °C while increased temperature shows a trend in decreased cell voltage by around 20 % at the maximum temperature of operation (Ahn et al., 2014; Pavel et al., 2014). AEMs optimally work at a pressure of 30 bars, while experimental and modeling work has been conducted at high pressures. The major problem of high-pressure operation has been reported to be the trapping of product gases in the MEA since highly compressed cell does not allow a path for H_2 and O_2 (Zhang and Zeng, 2012). The electrolyte is one of the most performance-influencing parts of the AEM, and the selection of the type of electrolyte based on the application is also crucial. KOH, deionized water, pure water, K_2CO_3 and $KHCO_3$ mixtures are used as electrolytes, while KOH shows the lowest resistance among all in a comparative study (Pavel et al., 2014). Another comparative work to study electrolyte resistances has been conducted for NaOH, Na_2CO_3, $NaHCO_3$, and deionized water and concluded that pH values are effective on internal resistances (Zeng and Zhao, 2015a). 0.1 M NaOH and Na_2CO_3 show lower voltages at higher current densities compared to others. Some other experimental works utilizing various electrolytes for performance improvement can be found elsewhere (Ahn et al., 2014; Parrondo et al., 2014; Xiao et al., 2012; Wu and Scott, 2012).

Since the AEM technology is new, there have been developments in different parts of the electrolyzer. Development of membranes and ionomers is underway with potential problems of their toxic nature, conductivity-related issues, and thermal/chemical stabilities (Ran et al., 2014; Li et al., 2015; Ren et al., 2014). Some research on electrocatalysts is also available that has been identified and assessed in (Tiwari et al., 2019). AEM technology requires further development for optimal operating conditions, better durability, and higher efficiencies to compete with existing methods, while it has a significant potential for being low-cost thanks to the use of non-noble catalysts. A great potential to reduce the size and weight of the electrolyzer by utilizing porous electrolytes is also an intensively studied option for AEM that phases out the use of liquid electrolytes and their circulation requirements, needing pumps and extra pump instalments (Li et al., 2020).

Table 3 shows the studies conducted in the literature for AEM water electrolysis comparatively. The studies were generally carried out in the temperature range of 50–70 °C and at ambient pressure. It has been observed that the electrolysis efficiency varies between 70 % and 80 %, and the energy consumption range is between 3.76 and 4.2 kWh/Nm^3. Although it is reported that there is a degradation of 500 μV/h and above in AEM water electrolyzer cells, there are studies with an assertive degradation amount of 0.7 and 5 μV/h (Motealleh et al., 2021; Liu et al., 2017).

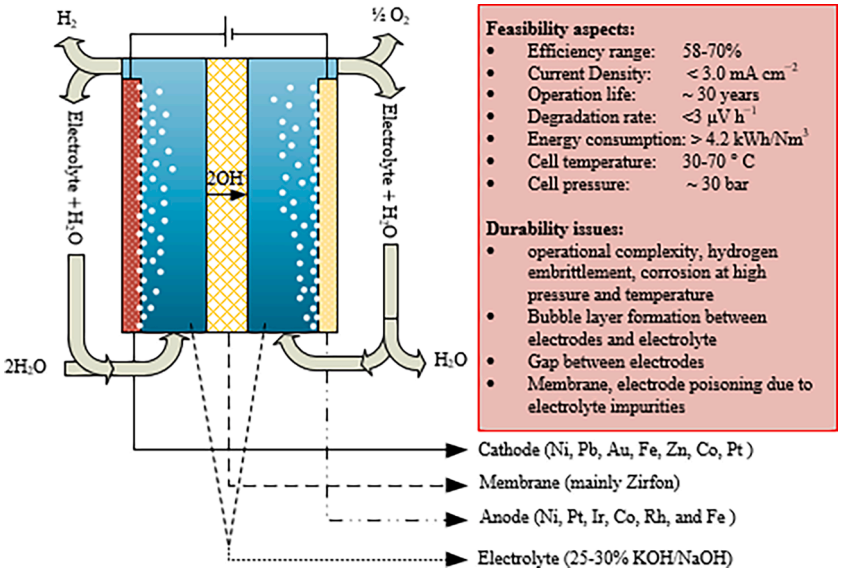


Fig. 2. Operational aspects and principles of Alkaline Electrolyser.

Table 2
Detailed comparison for alkaline water electrolysis studied in the literature.

Membrane (electrolyte/ separator)	Electrolyte Solution	Anode Catalyst/ Electrode	Cathode Catalyst/ Electrode	Cell Area (cm^2)	no of Cells	E (Volt)/ Cell	Current dens. (mA/ cm^2)	Cell Temp (°C)	Operational Life Test (h)	Reference
x	KOH	NiCu	Pt wire and a saturated calomel electrode	1.32	1	1.4	50	RT	x	(Ahn et al., 2013)
x	KOH	Nickel	Raney Nickel		1	1.76	400	80	x	(Manabe et al., 2013)
x	6 M KOH, NiCoMo	Nickel	Nickel	0.5	1	2,25 1,95				(Maslovara et al., 2013)
x	6 M KOH	Nickel	Nickel		1		100	70	x	(Marćeta Kaninski et al., 2013)
AAEMWE	1 M KOH	Ni on Carbon Paper	Nickel	10.24	1	1.9	150	x	x	(Ahn et al., 2014)
x	KOH	Nickel Foam ($SrTiO_3$ & Co-Mo)	Inconel Foam ($SrTiO_3$ & Co-Mo)	x	1	1.75	2230	250	150	(Allebrod et al., 2014)
anion selective (Dowex Marathon)	10 wt.% KOH	Fe doped $NiCo_2O_4$ Nickel foam	bare Ni	21.72	1	1.85	115	50	x	(Chanda et al., 2014)
x	6 M KOH	Pt	Porous Ni3Al–Mo	x	x	x	100	RT	120	(Wu et al., 2014)
Porous PES (polyether sulfone)	30 wt% KOH	Nickel foam	Pt coil	200	26	1.8	500	80	x	(Kim et al., 2015)
PVP:*K*+- Aquivion, PBI, Zirfon Pearl	30 wt% KOH	Polished Nickel plates	Polished Nickel plates	x	1	2.5	700	80	x	(Aili et al., 2015)
polysulfone with Sb2O5 or TiO2 filler	6 M KOH	Ni Mesh, Ni-Co coated	Ni Mesh, Ni-Co coated	900	1	1.85	600	85	500	(Kuleshov et al., 2016)
x	1 M KOH	nickel-coated copper	Cu/Ni/ NiZn–PtRu	2	1	x	100	RT	x	(Solmaz et al., 2016)
Zirfon	50wt% KOH	LaNiO3 doped Ni Mesh	Watts Ni	25	1	1.9	800	120	500	(Egelund et al., 2016)
L-ABPBI, C-ABPBI, Zirfon	30 wt% KOH	Ni Foam	Ni Foam	3.61	1	2	335	70	x	(Diaz et al., 2016)
x	1 M KOH	TiO2-NT-Ag & DLC doped	TiO2-NT-Ag & DLC doped	2	1	1.8	50	RT	120	(Baran et al., 2017)
Zirfon Perl UTP 500	1 M NaOH	Ni Foam	Ni Mesh	10	1	2.3	250	80	24	(Phillips et al., 2017)
qPPO/PTFE/ Nafion	10 wt% KOH	Ni Foam/ NiCo2O4	Bare Ni Foam	4	1	1.85	135	50	135	(Chanda et al., 2017)
x	1 M KOH	Ni3Se2/NF	NiCo2S4/NF	1.8	1	1.98	50	x	500	(Sivanantham and Shanmugam, 2017)
Asbestos, TiO2 composite	30 wt% KOH	Ni	Ni	10	1	2	300 600	80	100	(Shiva Kumar et al., 2018)
x	NaOH	Ti/TiO2RuO2	Ni	80	1	2.5	470	50	288	(Amikam et al., 2018)
x	6 M KOH	Raney nickel & cobalt spinel	Raney nickel/ Mo activated	200	5	1.9	1000	80	1000	(Kuleshov et al., 2019)
m-PBI, OPBI	6 M KOH/ 3 M H_2SO_4	Pt	Ru coated Ti	4	1	2	800	60	40	(Wan et al., 2021)

High-temperature steam electrolysis

High-temperature steam electrolysis (HTSE), also called solid oxide electrolysis cell (SOEC), is a high-temperature water electrolysis method with advantages such as high conversion efficiency, high reaction kinetics favored by high temperature, and low overpotentials. High-temperature operation enables the use of steam as the feed where its Gibbs free energy is lower than that of the liquid water, directly lowering the electricity consumption by almost 25 % while the remaining energy requirement is compensated by high-temperature heat higher than 800 °C (Laguna-Bercero, 2012; Pandiyan et al., 2019), while it can be decreased to lower temperatures (Wang et al., 2010). At higher voltages with overpotentials, stack efficiency is around 78 % at 1.6 V, which is well beyond other methods, while its electrical energy consumption is at a range of 2.9 – 5.0 kWh/Nm^3H_2 at current densities higher than 3 mA/cm^2 (Tang et al., 2018). Degradation characteristics are still not well known, while it is expected to be higher than 40 μV/h, and this significantly affects the operational life of the cell and stack, which could be as low as 5 years (Tietz et al., 2013). A high temperature is also required for enhanced conductivity of the oxygen ion electrolyte. A common electrolyte type for SOEC is yttria-stabilized zirconia (YSZ), while the oxygen electrode is made of lanthanum (LSM), and the cathode is made of nickel-based YSZ (AlZahrani, 2017). SOEC technology was first proposed as an alternative to conventional alkaline electrolysis in the mid-80 s and attracted a large interest with high efficiencies (Dönitz and Erdle, 1985). The Westinghouse Corporation has accomplished the most significant advances to the method, while many other institutions contributed to the development of SOEC (Yu et al., 2008; Bo et al., 2010; Warde et al., 1976; Cai et al., 2010; Quandt and Streicher, 1986; Erdle et al., 1992). Cell efficiency can reach up to 100 % Faraday

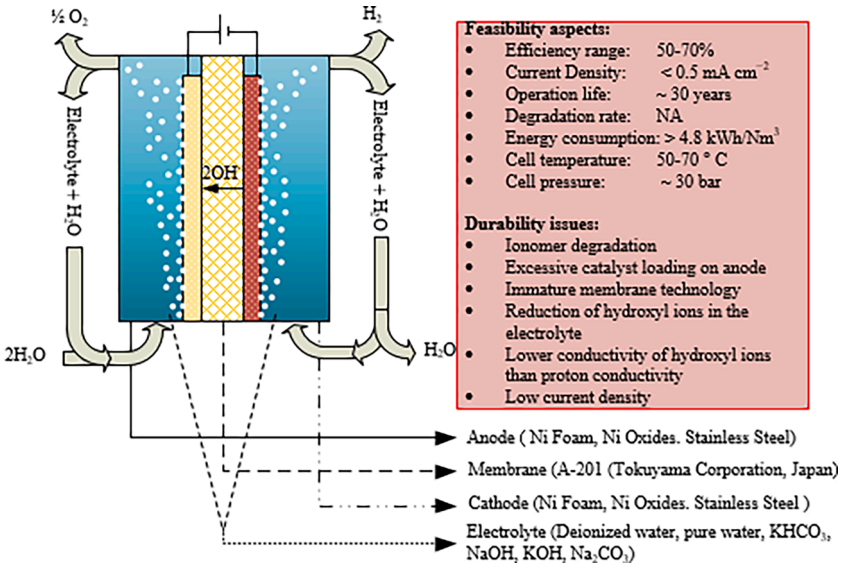


Fig. 3. Operational aspects and principles of a liquid electrolyte Anion Exchange Membrane electrolyzer.

efficiency, while high-pressure operation, non-noble catalysts, and a reasonable current density range make SOEC a promising alternative. Since SOEC can be used as a reversible fuel cell, which is a developed technology, most characteristics of the solid oxide fuel cell technology (SOFC) are also valid for SOEC (Maskalick, 1986; Fallah Vostakola et al., 2023). A general schematic of an SOEC cell is represented in Fig. 4.

The material development of the cell is parallel to those of SOFC technology and carries similar shortcomings and superiorities. As in the SOEC, its main components are an oxygen electrode as the anode, a fuel electrode as the cathode, and a solid-oxide electrolyte. The operational mode of the cell can be defined as endothermic, exothermic, and thermoneutral, where electricity consumption increases in the exothermic mode while heat requirement decreases, and vice versa occurs in the endothermic mode (Navasa et al., 2015). Perovskite composites such as Lanthanum strontium cobalt ferrite (LSCF) and strontium-doped manganite have been commonly applied to fabricate oxygen electrodes with high conductivity and lower ohmic losses. Even though their catalytic activities are suitable, unsuitable thermal expansion coefficients of materials may cause delamination. Some other materials are proposed to overcome such problems, such as lanthanum strontium ferrite (LSF) and co-dopped lanthanum silicate composites (Laguna--Bercero et al., 2010; Thomsen et al., 2009; Khan et al., 2020; Li et al., 2023). The combination of nickel, zirconia, and nickel with YSZ is mainly used for the fuel electrode at certain compositions for suitable thermal expansion and electronic conductivity, where nickel functions as the conductor and catalyst (Horri et al., 2012). Optimal mass transfer is also crucial for mass transfer, and therefore, triple-phase boundaries and electrode structure play a critical role in decreased activation and concentration overpotentials (Wang et al., 2021). Thermal expansion of fuel electrodes at high temperatures is also a crucial factor impacting cell performance, resulting in the delamination of the individual layers and leading to cell degradation. Such issues and possible ways to overcome them are comprehensively reviewed elsewhere (Shaikh et al., 2015). YSZ is used as the dense ceramic layer for electrolytes as mixtures of ZrO_2. It is the most widely accepted option as an electrolyte for SOEC since it meets certain requirements of a material to be used as an electrolyte, such as minimal thermal mismatch with electrodes, efficient electronic and ionic transport, and thermal/chemical stability (Nechache et al., 2014). Since YSZ ohmic conductivity is highly dependent on the cell temperature, lower temperature operation is impossible, while other materials such as $LaGaO_3$ and ceria fluorites are used as thin layers to reduce the operating temperature (Huang et al., 1996; Stojmenović and Dodevski, 2021). Even though different dopants, such as MgO and CaO are also used, YSZ is still the dominant electrolyte material in SOEC applications (Ni et al., 2008; Savoini et al., 1998; Wang et al., 2018). Cells and stacks are generally sealed with glass, while interconnect materials are generally noble materials such as platinum and gold for better electronic conductivity purposes (Kiebach et al., 2017). The materials studied for SOECs, including electrodes, electrolytes, and their essential coating layers, have been comprehensively reviewed elsewhere (Mahato et al., 2015; Faisal et al., 2022).

Degradation in SOEC cells is one of the most crucial aspects as it makes use of SOEC disadvantageous compared to other electrolysis systems, causing low operational life (Moçoteguy and Brisse, 2013). Degradation of a SOEC almost doubles that of a PEM electrolyzer, and many issues related to the high-temperature operation, such as delamination of layers and catalysts performance, need to be resolved before market penetration of SOEC systems (Chen, 2016). Chemical, electrochemical, structural, and mechanical degradation are major groups of cell degradation in SOEC stacks. There have been many reported experimental studies on voltage degradation of SOEC cells or stacks, where experimentation on the stack is a better option to represent losses due to mechanical and structural failures. Up to 9000 h of SOEC cell testing is accomplished where the rate of voltage degradation has been found to be 40 μV/h (Schefold et al., 2011). Some other studies reported that cell degradation accounts for 3.8 %/kh at 3600 h and 2 %/kh at lower operational hours (Hauch et al., 2008; Fang et al., 2013). At the stack level, the rate of degradation is even faster due to pollution on seals and interconnects and delamination between layer contact (Jones and Thomas, 2007). For a 25-stack cell operation, a 20 % current drop has been observed corresponding to 10 %/kh at 900 h operation (O'Brien et al., 2007). In another study for a 5-cell stack, voltage degradation was 7 %/kh for 3000 h of operation (Zahid et al., 2010). A 10-cell stack was also studied to evaluate the degradation rate, where 5.6 %/kh voltage degradation was observed (Zhang et al., 2013). At the stack level, the best-performing cell in terms of cell degradation has been reported to be 1.5 %/kh (Fang et al., 2013). Scaling up to stack level with a higher number of cells can cause irreversible damage on the stack, and voltage degradation also drastically increases (Léon et al., 2021). Factors that affect degradation mechanisms on cell and stack levels are comprehensively compiled elsewhere (Wang et al., 2020).

The design of SOEC is parallel or the same as the SOFC when used at reversible operating conditions. Therefore, the geometry of SOEC is the same as in SOFC. Planar and Tubular configurations are the most common SOEC cell geometries, while novel configurations such as flat tubular are also under the research phase (Tonekabonimoghaddam and

Table 3
Detailed comparison for anion exchange membrane water electrolysis studied in the literature.

Membrane	Electrolyte Solution	Ionomer	Anode Catalyst	Cathode Catalyst	Anode loading mg/cm^2	Cathode loading mg/cm^2	Anode Current Collector	Cathode Current Collector	Cell Area (cm^2)	E (Volt)/ Cell	Current dens. (mA/ cm^2)	Cell Temperature (°C)	Operational Life Test (h)	Reference
Fumapem FAA-3–50 (Fumatech) and Orion TM1	1 M KOH	30 wt%	IrO2	40 wt% Pt/C (Johnson Matthey)	3	0.6	Ti Felt (CNL Energy)	Carbon Paper (JNT40-A3)	5	1.9	2750	70	10	(Kang et al., 2022)
Fumapem FAA-3-PP-75 (Fumatech)	1 % K_2CO_3	9–30 wt% I2 (Acta Spa)	CuCoOx (Acta 3030®)	Ni/ (CeO2–La2O3)/C (Acta 4030®)	7.4	30	Ni foam (80–110 PPI; American Elements)	Microporous carbon paper (Fuel Cells Etc)	5	1.95	500	60	200	(Vincent et al., 2017)
x	1 M KOH	20 wt% FAA-3-Br (Fumatech)	IrO2 (Surepure Chemetals	40 wt% Pt/C (Johnson Matthey)	4	x	Ti	Graphite	5	1.9	1500	70	x	(Park et al., 2019)
Sustainion® 37–50, Fumasep FAS-50, Fumasep FAPQ, Neosepta ACM, AMI 7001, Nafion® 115, and Celazole® PBI.	1 M KOH	x	NiFe2O4 (Sigma Aldrich)	NiFeCo (US Nano)	2	2	x	Carbon Paper Sigracet 39BC GDL	5	1.9	1000	60	2000	(Liu et al., 2017)
AF1-HNN8–50	1 M KOH	Aemion™ (AP1-HNN8) and Fumion™ (FAA-3-SOLUT-10	Ir black (Alfa Aesar)	60 wt% Pt/C (Alfa Aesar)	3.8	3.8	Porous Ti	Toray 090	25	1.82	2000	60	1000	(Fortin et al., 2020)
Fumapem FAA 3–PE (Fumatech)	1 M KOH	Fumion FAA-3-SOLUT-10 (Fumatech)	Ir black (Alfa Aesar)	60 wt% Pt/C (Alfa Aesar)	5	5	Porous Ti (Beakaert)	Porous Ti (Beakaert)	25	1.75	1000	50	x	(Faid et al., 2018)
Fumapem FAA 3–PE (Fumatech)	1 M KOH	Fumion FAA-3-SOLUT-10 (Fumatech)	Ni90Fe10 and Ir black (Alfa Aesar)	60 wt% Pt/C (Alfa Aesar)	6	1	Porous Ti (Beakaert)	Porous Ti (Beakaert)	25	1.99	2000	50	x	(Cossar et al., 2019)
A201 (Tokuyama)	1wt. % K_2CO_3	x	CuCoOx (Acta 3030®)	CeO2-La2O3/C (Acta 4030®)	36	7.4	x	x	x	1.81	470	55	1000	(Pavel et al., 2014)
FAA-3-PK-130	0,1 M KOH	x	Graphene-nanoplatelets-supported (Ni,Fe)	MoNi4/MoO2	2.5	2.5	x	x	x	1.85	1150	70	1000	(Thangavel et al., 2020)
X37–50 Grade T	1 M KOH	x	Cu0.5Co2.5O4	40 wt% Pt/C (Johnson Matthey)	10	1	Ni Foam	Ni Foam	4.9	1.8	1300	50	100	(Jang et al., 2020)
A201 (Tokuyama)	0,5 M KOH	PTFE	IrO2 (Premion®, Alfa Aesar)	Pt/C (Pt 46.5 wt%, Tanaka K. K.)	x	x	Ti Plate	Graphite plate	6.25	1.8	1070	50	x	(Cho et al., 2018)

(*continued on next page*)

Table 3 (*continued*)

Membrane	Electrolyte Solution	Ionomer	Anode Catalyst	Cathode Catalyst	Anode loading mg/cm^2	Cathode loading mg/cm^2	Anode Current Collector	Cathode Current Collector	Cell Area (cm^2)	E (Volt)/ Cell	Current dens. (mA/ cm^2)	Cell Temperature (°C)	Operational Life Test (h)	Reference
FAA-3–50 (Fumatech)	1 M KOH	Fumion FAA-3-SOLUT-10 (Fumatech)	IrO2/NiFe	40 wt% Pt/C (Johnson Matthey)	2	0.4	Porous SS	Porous SS	5	1.9	2760	50	3	(Park et al., 2022)
FAA-3-PK-75 (Fumatech)	0,5 M KOH	x	IrO2 (Premion®, Alfa Aesar)	Pt/C (Pt 46.5 wt%, Tanaka K. K.)	x	x	Titanium paper (250 μm, Bekaert)	Carbon paper (TGP-H-120, Toray)	6.25	1.8	983	90	x	(Lim et al., 2019)
FAA-3–50 (Fumatech)	1 M KOH	Fumion FAA-3-SOLUT-10 (Fumatech)	Fe0.2Ni0.8-P0.5S0.5	Fe0.2Ni0.8-P0.5S0.5	3.2	3.2	Ni Foam	Ni Foam	5	2	2500	60	x	(Wan et al., 2022)
Sustainion® 37 (Dioxide Materials)	1 M KOH	x	IrO2/CP (Dioxide Materials)	Ni@Ni(OH)2/Ti	x	0.83	x	x	1	2	1000	50	x	(Guo et al., 2022)
FAA-3–50 (Fumatech)	1.0 M KOH + 1.5 M EtOH	x	Ni/540	Ni/540	0.35	0.35	Carbon GDL	Carbon GDL	5	2	435	RT	x	(Guo et al., 2022)
FAA-3PE-30 (Fumatech)	1 M KOH	Fumion FAA-3-SOLUT-10 (Fumatech)	Ni90Fe10 / Ni80Fe20 / CeO2	60 wt% Pt/C (Alfa Aesar)	5	1	Gold coated porous titanium	Gold coated porous titanium	25	1.72	800	50	12	(Cossar et al., 2021)
Sustainion® X37–50 (Dioxide Materials)	1 M KOH	x	NiFe2O4 (US Research Nanomaterials)	Raney nickel (Sigma Aldrich)	2	3	SS GDL	Nickel fiber paper (Dioxide Materials)	5	1.85	1000	60	12,000	(Motealleh et al., 2021)
Fumapem-3-PE-30	1 M KOH	Fumion FAA-3	Ni0.6Co0.2Fe0.2	60 wt% Pt/C (Alfa Aesar)	5	1	Au coated Ti felt (Bekaert)	Carbon paper (Toray)	25	2	1500	50	x	(Faid et al., 2022)
FAA-3–50 (Fumatech)	1 M KOH	x	5 wt%CdS/ZIF-67	Pt/C (46.7 wt%, Tanaka Kikinzoku)	3	1	GDL	GDL (AvCarb, MGL190)	9	1.85	1000	60	x	(Devarayapalli et al., 2022)
FAA-3–50 (Fumatech)	1 M KOH	Fumion FAA-3	NiFe	Ni	0.35	0.38	Carbon Paper	Carbon Paper	5	2	600	60	40	(López-Fernández et al., 2022)
Fumapem-3-PE-30	1 M KOH	Fumion FAA-3-SOLUT-10 (Fumatech)	Ir black (Alfa Aesar)	60 wt% NiCu MMO/Ketjen black	3	5	Ti felt (Bekaert Inc.)	Carbon paper (Toray 090)	25	1.7	1800	50	x	(Faid et al., 2021)
A201 (Tokuyama)	K_2CO_3 or KOH	x	CuCoOx	Pt/C (TEC10V50E, TKK)	4.2	3.5	Ni foam (Celmet, Sumitomo Electric)	Carbon paper (Toray 090)	25	1.7	1000	50	x	(Ito et al., 2018)
A201 (Tokuyama)	1 M KOH	x	Ni	Pt-Ni	$2{,}85\times10^{-3}$	$1{,}85\times10^{-3}$	Carbon paper (Toray 090)	Carbon paper (Toray 090)	4	1.9	250	70	x	(Ahn et al., 2016)
Mg-Al LDH	0.1 M NaOH	x	CuCoOx (Acta 3030®)	CeO2-La2O3/C (Acta 4030®)	40	40	Ni Foam (Hohsen)	Carbon paper (E-TEK)	3.14	2.2	208	70	600	(Zeng and Zhao, 2015b)
Sustainion® X37–50 (Dioxide Materials)	1 M KOH	x	Fe-NiMo-NH3/H2	NiMo-NH3/H2	2.5	2.5	Carbon paper	Carbon paper	x	1.57	1000	80	x	(Chen and Hu, 2020)

(*continued on next page*)

Table 3 (*continued*)

Membrane	Electrolyte Solution	Ionomer	Anode Catalyst	Cathode Catalyst	Anode loading mg/cm^2	Cathode loading mg/cm^2	Anode Current Collector	Cathode Current Collector	Cell Area (cm^2)	E (Volt)/ Cell	Current dens. (mA/ cm^2)	Cell Temperature (°C)	Operational Life Test (h)	Reference
DURAION (Evonik Industries)	1 M KOH	DURAION (Evonik Industries)	Ni3Fe LDH	Pt/C	2	0.6	Ni fiber	Carbon paper	5	2	2070	55	400	(Jiang et al., 2022)
x	1 M KOH	x	NiFeCr LDH	V-Ni2P/Ni12P5	2	2	x	GDL	x	1.79	500	55	40	(Zhao et al., 2022)
Sustainion® X37–50 (Dioxide Materials)	1 M KOH	x	NiFeV LDH	Pt/C	3.95	x	Ni Foam	Carbon cloth	4.9	1.8	2100	50	x	(Lee et al., 2021)

Shamiri, 2021). Planar configurations are more common, with advantages such as a short current collection path and high volumetric density, while tubular configuration phases out sealing problems and higher cell mechanical and thermal stability (Zheng et al., 2017). They can be classified as self- or external-supported cells, while self-supported cells can be electrolyte-, anode-cathode-, and interconnect-supported (Ho et al., 2009). Compared multi-dimensional models have been developed while not much difference in their electrical efficiencies was obtained (Stiller et al., 2005). Some other various geometries, such as honeycomb, micro-tubular, and single-chamber configurations, and their aspects can be found elsewhere (Mohammadzadeh et al., 2020; Fallah Vostakola and Horri, 2021).

Table 4 shows comparatively the studies conducted in the literature for high-temperature steam electrolysis. The studies were generally carried out in the temperature range of 700–900 °C and at ambient pressure. Although a wide degradation range has been observed in HTSE cells, there are studies with successful degradation values of 3 μV/h (Schefold et al., 2020).

Electrochemical water splitting – a clean approach

An entirely clean hydrogen production approach is only possible when the hydrogen generation facility, equipment, and relevant logistics do not utilize fossil-based energy sources throughout their whole lifetime operation. Routes of completely clean hydrogen production have been represented in Fig. 5. In this case, even if biomass is considered a renewable energy source, it is not included in the green hydrogen methods due to intensive emission potential even though it is within the natural Carbon cycle. Some review studies have analyzed the hydrogen production methods and recent advances in general (Dincer and Acar, 2015), based explicitly on a certain technique (Mehrpooya and Habibi, 2020; Oruc and Dincer, 2021; Fallah Vostakola et al., 2022), material specifications and characteristics (Roeb et al., 2012), or high-temperature solar thermal applications (Steinfeld, 2005; Ozcan et al., 2022). There are also a few review records with various assessments of hydrogen generation routes, their economics, and environmental aspects (Acar and Dincer, 2014; Mueller-Langer et al., 2007; Bhandari et al., 2014; Cetinkaya et al., 2012; Ferrero et al., 2013; Guban et al., 2020; Ozbilen et al., 2013).

One of the interesting pathways to produce clean hydrogen is to integrate solar photovoltaic cells and wind power with various PEM, AE, and AEM electrolyzers. In the case of SOEC, a hybrid combination of concentrated solar power (CSP) and renewable electric power would make a clean approach for water splitting. Solar PV efficiencies are the major limitation for low hydrogen efficiencies of PV-electrolysis systems due to low maximum reachable efficiencies in PV technology (Christopher and Dimitrios, 2012). PV-electrolysis systems show an efficiency range of 4.5 % to 18 % based on the type of electrolysis and PV technology as well as the availability of solar irradiance and location (Schüttauf et al., 2016; Khelfaoui et al., 2021; Burhan et al., 2017; Yang et al., 2015). There is also a significant difference between experimental studies, modeling work, and available systems. CSP technology has higher thermodynamic efficiencies and better performances when integrated with highly efficient SOEC technology, where hydrogen efficiency with CSP-SOEC couples can be as high as 45 % (Kaleibari et al., 2019; He et al., 2020; AlZahrani and Dincer, 2016). One of the challenges with CSP is occupying large lands, tracking requirements, and high capital costs due to little penetration in the market. Wind energy is one of the green methods that can be used as the source for low-temperature water electrolysis. The highest possible electrical efficiency of a vertical wind turbine does not exceed 59 % due to the Betz limit; however, its performance is higher than PV technology overall. Wind-driven hydrogen production has the potential to have as high as ~45 % depending on the wind turbine-electrolysis couple, while a significant decrease is observed when energy storage is considered to prevent intermittent operation. Since it does not provide

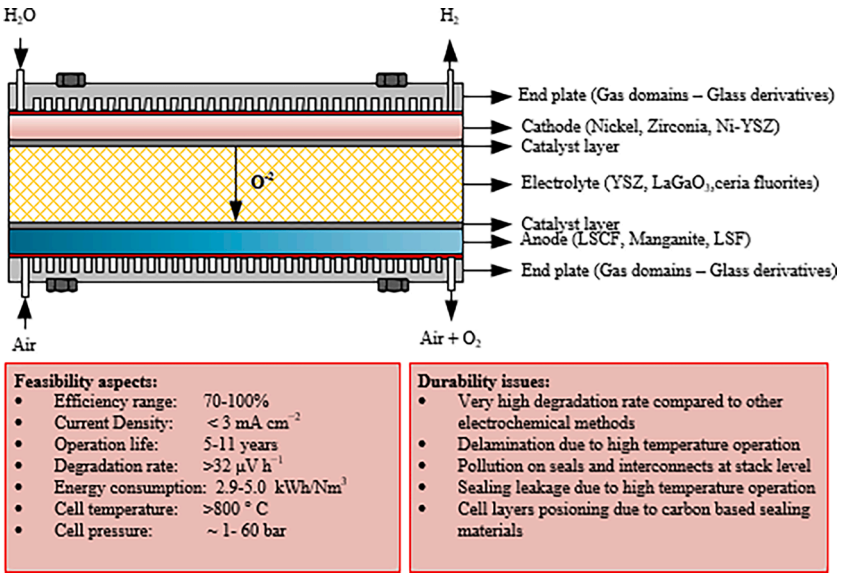


Fig. 4. Schematics and operational principles of high-temperature steam electrolysis.

high-temperature heat, an additional source of high-temperature energy is required from another source to couple wind energy to SOEC with hybrid technologies (Nakken et al., 2006; Ishaq et al., 2018; Alavi et al., 2016; Saur and Ramsden, 2011).

Even though its energy density is low and high capital investments are required, hydro-energy is one of the most efficient and cost-effective renewable energy technologies available in most parts of the world. Various types of turbine technologies have successfully been developed and are under use through various dam heights. Hydrogen efficiency from hydroelectricity-driven electrolysis systems can be as high as 80 % and is one of the most cost-effective options among green hydrogen technologies (Christopher and Dimitrios, 2012; Padilha et al., 2009; Bamisile et al., 2020; Lee et al., 2020; Bødal and Korpås, 2020). Geothermal energy-driven hydrogen generation is another cost-effective solution for green hydrogen generation where high-temperature geothermal sources are also utilized for heating purposes of high temperature requiring hydrogen splitting technologies such as SOEC. Higher temperature heat is also achievable with chemical heat pump use as a state-of-the-art technology (Rafferty, 1999; Kato et al., 1999; Kato et al., 1997; Wongsuwan et al., 2001; Dincer and Ozcan, 2018). Geothermal power technologies such as single-flash, multi-flash and binary systems have efficiencies below 20 %. Therefore, coupled performances are also not comparable to those of hydro- and wind-based technologies, and the availability of geothermal sources depends on the geological structure of the location. However, geothermal energy-driven electricity generation is very cost-competitive and may lead to cost-effective green hydrogen solutions with matured hydrogen energy systems (Dincer and Ozcan, 2018; Ghazvini et al., 2019; Balta et al., 2009). Nuclear energy is another source of clean energy for water electrolysis, and its availability is based on the availability of technology. Almost all nuclear power plants run with pressurized water reactor technology with a maximum temperature of 310 °C and an efficiency range of 28–34 %. Low-temperature water electrolysis systems can work at an efficiency range of 18–30 % with nuclear electricity. Next-generation nuclear reactor technologies with higher maximum operating temperatures show the potential to be highly efficient, such as next-generation Canadian Deuterium Uranium (CANDU) reactors, high-temperature gas reactors, and molten salt reactors (El-Emam and Özcan, 2019; El-Emam and Bhattacharyya, 2021; El-Emam et al., 2015a).

Several works have reported the performances of the other less-common sources of renewable-driven electrolysis units, such as tidal/wave energy, hydropower, and geothermal units (Serna and Tadeo, 2014; Temeev et al., 2006; Di Dio et al., 2009). Considering the readiness level of the technology and feasibility aspects, the hydropower-AE coupled units can comparably provide hydrogen at a higher efficiency. However, the pilot plants deployed based on the wind- and solar PV-electrolyser units are more common than the location-dependent hydro- and geothermal-based units. Increased technology maturity of increased durability of electrolysis systems presents a great potential to be employed for the ambitious zero-emission targets. Novel technologies, intensive research on catalysts, and experimental and modeling works on newly developed materials are present in the recent literature giving a hint that increased operational life, decreased durability issues, and more efficient operation are on the way for an efficient, cost-effective and zero/low carbon hydrogen era.

Clean hydrogen as a strategy for net-zero targets

Deploying efficient production methods to deliver green hydrogen is crucial to achieving the net-zero objectives. However, the economy of the production process is even more critical when it comes to deployment at a large scale compatible with capital expenses and low production costs to compete with existing grey-hydrogen platforms. There have been recent initiatives for carbon taxing in certain countries, which in turn could bring an extra cost load on hydrogen generation technologies with carbon emissions that leads to increased interest in zero-emission green hydrogen technologies (Knobloch et al., 2019). Here, the economics of green hydrogen technologies are discussed, their environmental and safety aspects are summarized, and penetration of green hydrogen into the market is investigated. The levelized cost of hydrogen from grey hydrogen technologies amounts to USD 0.80 – 1.50 /kg H_2, while green technologies, mainly with PEM and AE technology, range between USD 3.00 – 8.00 /kg H_2 in existing facilities. Even though the cost of hydrogen from renewable electrolysis decreased by almost 40 % since the beginning of the millennium, it is still high compared to fossil-based technologies. The near-term projections represent a further decrease of 60 % after the deployment of national strategies and market penetration acceleration with decreased capital expenditures (CAPEX) (Council, 2020). It is also reported that hydrogen utilization in mobile applications may bring 1.5 to 2 times more cost load to end users. This value multiplies by eight if it is used for synthetic fuel production for aviation applications (Ruth et al., 2020). It is also crucial to investigate the costs and issues related to hydrogen infrastructure, energy losses through production and transportation due to low efficient applications

Table 4
Detailed comparison for high-temperature steam electrolysis studied in the literature.

Electrolyte	Cell structure	Anode Catalyst	Cathode Catalyst	Anode Current Collector	Cathode Current Collector	Cell Area (cm^2)	Number of Cells	E (Volt)/ Cell	Support	Feed gas	Electrode polarization resistance Rp (ohm cm^2)	Current dens. (mA/ cm^2)	Cell Temperature (°C)	Operational Life Test (h)	Reference
SDC	LSCM-GDC	half-cell	LSCM-GDC	Pt paste	Pt paste	0.25	1	(−0,1)	Electrol. (0.75 mm)	(4 % H_2O/ H_2)	0,206–2181	2360	800	x	(Huang et al., 2022)
Gd0.1Ce0.9O2-δ	SSF-GDC/ GDC/YSZ/ GDC/SSF-GDC	Sm0.5Sr0.5FeO3-δ	Sm0.5Sr0.5FeO3-δ	x	x	x	1	2	Electrol.	x	0.11	1560	800	25	(Ling et al., 2022)
YSZ	BSCFTa/ YSZ/ BSCFTa	BaSrCoFeTa	BaSrCoFeTa	Pt mesh and paste	Pt mesh and paste	0.19	1	1.8	Electrol.	x	0.02	450	800	80	(Prasopchokkul et al., 2021)
8 %Y2O3-ZrO2 (YSZ, TZ-8Y, Tosoh)	PSTF/ YSZ/LSM-YSZ	LSM-YSZ (Ningbo SOFCMAN Energy)	Pr0.3Sr0.7Ti0.3Fe0.7O3−δ	Ag paste and Ag wire	Ag paste and Ag wire	0.12	1	2	Electrol. (400 μm)	60 % H_2O/ Ar	0.43	934	850	20	(Zhang et al., 2017)
YSZ	LSTO/ YSZ/LSM-YSZ	LSM-YSZ	La0.3Sr0.7TiO3+δ	Gold	Gold	3.14	1	1.5	Electrol. (2 mm)	47 % H_2O/ N2	1.4	90	900		(Tsekouras and Irvine, 2011)
YSZ (SINOPHARM Chemical)	LSTC-SDC/YSZ/ LSM-SDC	LSM-SDC (SINOPHARM Chemical)	(La0.2Sr0.8) 0.9Ti0.9Cu0.1O3−δ	Silver wire (0.4 mm in diameter) and conductive adhesive	Silver wire (0.4 mm in diameter) and conductive adhesive	1	1	2	Electrol. (2 mm)	5 % H_2O/ Ar	1.5	159	800	24	(Qi et al., 2014)
YSZ	LSTN-SDC/YSZ/ LSM-SDC	LSM-SDC	(La0.3Sr0.7) 0.9Ti0.9Ni0.1O3−δ	Silver wire (0.4 mm in diameter) Silver paste (SS-8060, Xinluyi)	Silver wire (0.4 mm in diameter) Silver paste (SS-8060, Xinluyi)	1	1	2	Electrol. (2 mm)	3 % H_2O/ Ar	4.3	101.8	800	x	(Zhang et al., 2014)
YSZ	LSNTO/ YSZ/LSM-YSZ	(La0.8Sr0.2)0.95MnO3 (LSM)-YSZ	La0.4Sr0.4Fe0.06Ti0.94O2.97	x	x	25	1	1.5	Electrol. (2 mm)	47 % H_2O/ N_2	1.5	90	900	x	(Tsekouras et al., 2013)
YbScSZ	LSCM/ YbScSZ/ LSCM	La0.75Sr0.25Cr0.5Mn0.5O3−δ	La0.75Sr0.25Cr0.5Mn0.5O3−δ	Gold	Gold	3	1	1.7	Electrol. (165 μm)	50 % H_2O/ Ar	x	780	850	x	(Torrell et al., 2015)
YSZ	LSCM-Ni-SDC/YSZ/ LSCM-SDC	LSCM-SDC	Ni-loaded La0.75Sr0.25Cr0.5Mn0.5O3−δ	silver wire (0.1 mm in diameter) and silver paste (SS–8060 Xinluyi)	silver wire (0.1 mm in diameter) and silver paste (SS–8060 Xinluyi)	3.14	1	2	Electrol. (2 mm)	3 % H_2O/ Ar	3.4	80	700	x	(Li et al., 2013)
YSZ	LSCM-Fe-SDC/YSZ/ LSCM-SDC	LSCM-SDC	Fe-loaded La0.75Sr0.25Cr0.5Mn0.5O3−δ	silver wire (0.1 mm in diameter) & silver paste	silver wire (0.1 mm in diameter) & silver paste	3.14	1	2	Electrol. (2 mm)	3 % H_2O/ Ar	2.5	100	800	x	(Xu et al., 2013)
YSZ	LSCNNi-YSZ|YSZ| LSM-YSZ	LSM-YSZ	(La0.75Sr0.25)0.95 (Cr0.8Ni0.2)0.95Ni0.05O3−δ	silver wire (0.1 mm in diameter) and silver paste (SS-8060, Xinluyi)	silver wire (0.1 mm in diameter) and silver paste (SS-8060, Xinluyi)	1	1	1.5	Electrol. (1 mm)	3 % H_2O/ Ar	8.65	60	800	x	(Xu et al., 2014)

(*continued on next page*)

Table 4 (*continued*)

Electrolyte	Cell structure	Anode Catalyst	Cathode Catalyst	Anode Current Collector	Cathode Current Collector	Cell Area (cm^2)	Number of Cells	E (Volt)/ Cell	Support	Feed gas	Electrode polarization resistance Rp (ohm cm^2)	Current dens. (mA/ cm^2)	Cell Temperature (°C)	Operational Life Test (h)	Reference
8YSZ	YDC-LSCF/ 8YSZ/NiO-YSZ	NiO-YSZ	YDC-LSCF	(Co,Mn)3O coated Crofer 22 APU	(Co,Mn)3O coated Crofer 22 APU	100	3	1.3	Electrol. (5 μm)	90 % H_2O/ 10 % H_2	x	1000	800	1000	(Mougin et al., 2012)
YSZ	LSCF-GDC/YSZ/ Ni-YSZ	Ni-YSZ	LSCF-GDC	Inconel	Inconel	x	320	1.295	Anode	90 % H_2O/ 10 % H_2	x	1000	740	x	(Aicart et al., 2022)
YSZ	LSCF/ YSZ/Ni-YSZ	Ni-YSZ	LSCF	x	x	100	80	1.225	Anode (700 μm)	90 % H_2O/ 10 % H_2–N_2	x	410	750	1000	(Zhang et al., 2015)
Sr2Fe1.5Mo0.5O6−δ	SFM/ YbScSZ/ SFM	Sr2Fe1.5Mo0.5O6−δ	YbScSZ	Pt paste and Pt mesh	Pt paste and Pt mesh	3.5	1	1.3	Electrol. (280 μm)	90 % H_2O/ 10 % Ar	0.45	1400	900	24	(Bernadet et al., 2020)
La0.9Sr0.1Ga0.8Mg0.2O3	SFM/ LSGM/ SFM	Sr2Fe1.5Mo0.5O6−δ	Sr2Fe1.5Mo0.5O6−δ	Platinum paste (Haraeus CL11–5349)	Gold paste (Haraeus C8829)	0.33	1	1.3	Electrol.	60 % H_2O/ 40 % H_2	0.26	880	900	100	(Liu et al., 2010)
La0.8Sr0.2Ga0.87Mg0.13O3	SFM-SDC/ LSGM/ SFM-SDC	Sr2Fe1.5Mo0.5O6-Sm0.2Ce0.8O1.9	Sr2Fe1.5Mo0.5O6-Sm0.2Ce0.8O1.9	Au paste	Au paste	0.33	1	1.3	Electrol.	16 % H_2O/ 16 % CO_2/ 20 % H_2/48 %N_2	0.48	734	850	103	(Wang et al., 2016)
LSGM	SFMFe-LSGM/ LSGM/ SFM-LSGM	Sr2Fe1.6Mo0.5O6-δ	Sr2Fe1.6Mo0.5O6-δ	Silver paste	Silver paste	1	1	1.6	Electrol.	50 % H_2O/ 50 % CO_2	0.29	1270	850	x	(Hou and Xie, 2019)
6Sc1CeSZ	Ni-GDC/ 6Sc1CeSZ/ LSCF	Ni-GDC	LSCF	Pt Grids	Ni Grids	45	1	1.33	Electrol.	75 % H_2O/ 25 % H_2	x	900	850	23,000	(Schefold et al., 2017)
3YSZ	Ni-GDC/ 3YSZ/ LSCF	LSCF	Ni-GDC	Pt Grids	Pt Grids	128	x	1.23	Electrol. (90 μm)	H_2O/ H_2	0.5	700	856	5800	(Schefold et al., 2020)

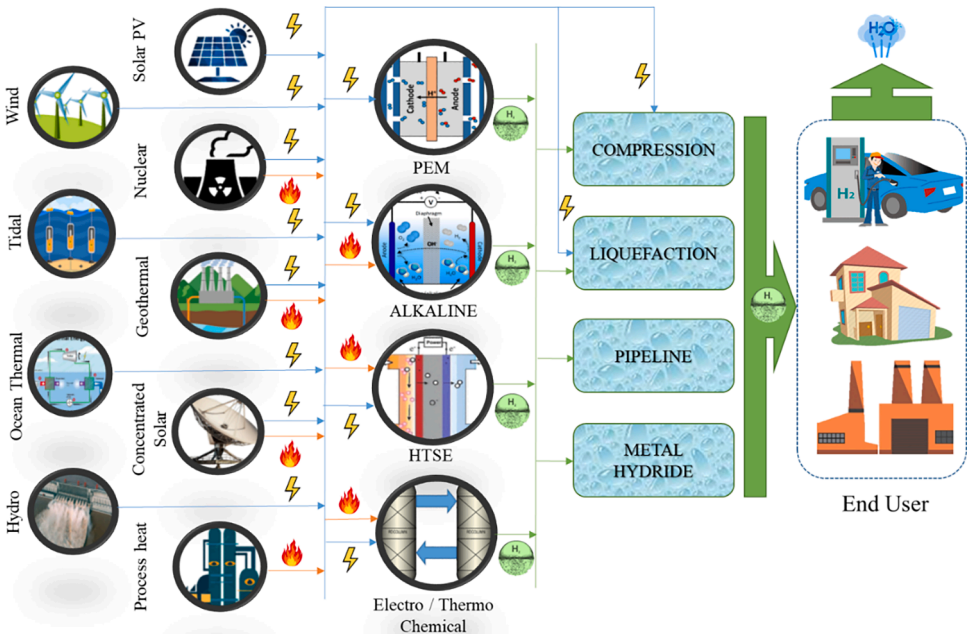


Fig. 5. Clean hydrogen routes with electrochemical water splitting.

and its high potential for leakage, and value recognition of green hydrogen by the energy sector. A recent report has been published by the International Renewable Energy Agency (IRENA) to point out issues related to green hydrogen as a guide to policy-making for net-zero targets (Bianco and Blanco, 2020).

Levelized cost of hydrogen

Electrolysis technologies are on-the-shelf hydrogen generation methods and ready to deploy for green hydrogen generation. A recent study compared solar, wind, and nuclear-driven low-temperature electrolysis (PEM and AE) to SMR in terms of their technology readiness level (TRL) (Al-Qahtani et al., 2021). TRL for green PEM and AE represent the same level as SMR, while the lowest TRL are evaluated as biomass-driven hydrogen generation with CCS. It is depicted that environmental externalities may represent a large percentage of total hydrogen costs. PEM and AE technology is already on the market, with further developments on the way. Decreased electricity consumption with novelties in electrolysis possess the potential to be competitive - even more cost-effective – to fossil-driven technologies. To compare the cost aspects of hydrogen production, it is essential to take into account the size of the plant, i.e., if a large- or small-scale plant is required for the demand. Developing the blue-hydrogen systems combining the SMR and the CCS units is still more economical if a large-scale production plant is favored. In contrast, for small-scale to mid-size plants, a decentralized water-splitting system based on integrated modular electrolyzer units can be a better choice (Zohuri, 2019).

The cost of electricity is the primary variable contributing to the cost of hydrogen production from water electrolysis, which may account for 47–78 % (Drive, 2017). Therefore, low-cost electricity sources are critical to achieving those target hydrogen costs set by various institutions (Yu and Yi, 2018). Some recent works report an extensive range of hydrogen production using renewable electricity to be between USD 2.28 – 7.43 /kg H_2 from various countries, and none of the options shows better cost performance than those of SMRs (Ewing et al., 2020; Blanco et al., 2018; Milani et al., 2020; Yu et al., 2021). Since there are not many industrial applications of renewable-driven hydrogen generation facilities, most of the studies reported in this field are based on fundamental techno-economic analysis and process simulation modules for cost estimation. Some other examples of cost estimation tools include the Hydrogen Economy Evaluation Program (HEEP) (Khamis, 2011), the MS Excel-based hydrogen analysis tool (H2A) developed by the Department of Energy in the US (James et al., 2016), National Renewable Energy Laboratories (NREL)'s H2FAST cost estimation software (Melaina et al., 2015), and another MS Excel-based tool developed by the Generation IV International Forum (GIF)'s G4Econs (Williams, 2007), with the latter one has particularly been designed for cost estimation of the nuclear-driven thermochemical hydrogen generation units. Financial tools such as economic, thermoeconomic, and exergoeconomic analyses are also primarily utilized for hydrogen cost estimation. Some recent screening works complied hydrogen generation costs, and other economic aspects from various sources can be found elsewhere (El-Emam and Özcan, 2019; Bartels et al., 2010a; Lemus and Duart, 2010a; Evans et al., 2009; El-Emam and Gabriel, 2021; El-Emam and Dincer, 2015; El-Emam and Dincer, 2014; El-Emam et al., 2014; El-Emam and Dincer, 2018).

The Wind-driven PEM electrolysis units can produce green hydrogen at a levelized cost ranging from USD 5.27 to 9.37 /kg H_2, varying with the plant capacity and selection of the wind energy technology (Saur and Ramsden, 2011; Olateju et al., 2016; Olateju et al., 2014; Choi et al., 2005a). A study conducted for a 50-ton/day wind-driven hydrogen plant with PEM using offshore wind platforms reported ~USD 6.00 / kg H_2 (Saur and Ramsden, 2011). Solar PV applications are also primarily coupled with the PEM electrolyzers, where the cost range from solar PV–PEM coupled units is reported as USD 6.35–12.6 /kg H_2. Higher costs are due to battery use for the steady operation of the plant and high capital investment costs (Choi et al., 2005a; Shaner et al., 2016). Integration of the solar PV cells with the AE units also shows a similar trend for hydrogen production cost (Greiner et al., 2007). A recent study shows a higher cost (USD 18.67 /kg H_2) could be associated with water electrolysis if integrated into the battery storage systems (Hinkley et al., 2016). This figure is predicted to be significantly decreased to below USD 10.00 /kg H_2 in the next decade. PEM and AE technologies can directly be electrified with existing nuclear technologies (mainly PWR) and large-scale production with stationary operation possibilities. These advantages also bring lower hydrogen costs when nuclear electricity is utilized. The cost of hydrogen produced through the Nuclear PWR-driven PEM and AE electrolyzers has been reported to be between USD 3.50–5.46 /kg H_2, which is significantly lower than those of wind-driven and solar-driven options (El-Emam and Khamis, 2017).

However, it should be noted that decreasing material costs and maturing renewable technologies by phasing out intermittency problems can decrease renewable hydrogen costs to levels competitive to nuclear-driven technologies since the investment costs for nuclear power plants do not seem to decrease in short/near terms and there are strategies to phase out the use of nuclear energy. SOEC technology is generally assessed with next-generation nuclear reactors and concentrated solar energy sources due to its high-temperature requirement. Using a solar dish-Stirling source for thermal energy/electricity feed for SOEC resulted in ~USD 16 /kg H2 in an early work (Bartels et al., 2010a) while using solar tower technology decreased the cost below ~USD 10 /kg H_2. With high-temperature nuclear technology use, hydrogen cost falls in the range of USD 2.24–3.73 /kg H_2, which is a significant decrease only if it could be deployed in short terms (El-Emam and Khamis, 2017; Yang et al., 2008). Cost assessment studies conducted for the SOEC technology are considered topical compared to PEM and AE-based hydrogen cost reports since the technology deployment for both the source and hydrogen generation system has not yet been accomplished fully, and the values provided can be considered as preliminary estimations.

In the UK, the cost of electricity from renewables is recently becoming more and more competitive with conventional power generation technologies, while high-temperature heat is still considered costly due to the requirement of developing technologies (Menegaki, 2008). A comparison of the pre-tax levelized cost of electricity (LCOE) from the UK electricity market is represented in Fig. 6 (Department for Business, E.a.I.S.B 2016; DiPippo, 2016; Parrado et al., 2016). The predictions for the next decade indicate a decrease in the LCOE from renewable sources with an increase in the price of grey hydrogen due to the requirements for infrastructure refurbishment for integrating the available SMR plants with the CCS units. Fig. 7 represents the cost reported in the literature using various electrochemical technologies driven by nuclear, solar, and wind energy for clean hydrogen production.

Hydrogen strategies and projects worldwide

Today about 94 % of the total emission reductions worldwide have been accomplished by deploying renewable energy sources (RES) over the past two decades. Nearly 2500 GW of RES was just installed in 2020, and this figure kept growing exponentially afterward (Taibi et al., 2020). As a chemical storage vector and the most efficient fuel, green hydrogen can significantly contribute to the deep decarbonization of power plants and potentially replace fossil fuels in the long term (van Renssen, 2020). Its deployment, however, depends on many factors, such as governmental policies, long-term budgets, stakeholder interests, and the local availability of renewables. The EU is one of the world's leading regions with tremendous RES system projects coupled with water electrolysis units (Commission, 2018). It is predicted that by blending green hydrogen (up to 20 %) with natural gas through the existing grid, the CO2 emissions relevant to industrial and household activities based on natural gas can be reduced to 6.5 % overall. Since green hydrogen production is entirely dependent on RES, the availability of electric power generated from RES is essential to achieve the net-zero target. To electrify all the energy sector with renewable hydrogen in the EU region, about 3600 TWh of electricity per year will be required in the short term (Birol, 2019b). Therefore, countries likely lack adequate RES to import either green electricity or hydrogen to fulfill their net-zero targets. This would initiate a new era led by the hydrogen economy at the center of the global market and a driving force to achieve sustainable growth and development worldwide. The developing countries can also benefit from having natural renewable sources, such as those with potential solar sources in North Africa, from boosting their economies with necessary investments financed by neighboring nations with necessary technologies. Because of low operational costs in developing countries, low-cost hydrogen generation is possible in the near future, with many other opportunities and partnerships for a green hydrogen economy. Today's grey hydrogen is also the cheapest, followed by blue and green hydrogen, while carbon taxing approaches above USD 70 per ton. This could make blue hydrogen more economical than grey hydrogen. Carbon taxing issues are currently under review by the local governments in most countries around the world (Peters et al., 2020).

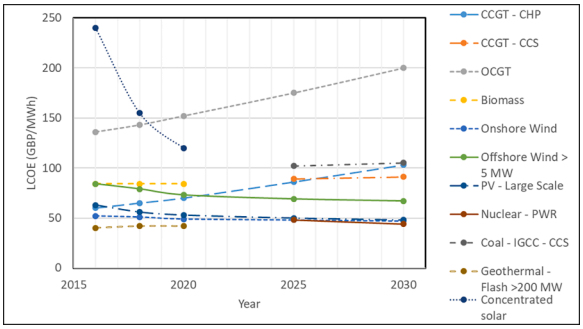


Fig. 6. Estimated LCOE from different sources in the UK.

Since water electrolysis has already accessed the market and reached confident readiness and maturity, it is considered an essential add-up to many prospective hydrogen plants for large-scale renewable energy projects. Integrating the CCS technology into the existing grey hydrogen plant is also under review by many countries. The UK has already planned to install 30 GW of offshore wind energy to electrify the energy sector. The installation capacity will contribute to supplying thousands of mini combined heating and power (CHP) systems for district heating of residents, large fuel cell systems for extra energy storage and utilization, and the blended hydrogen-natural gas grid plan (Phillips and Fischer, 2021). The US also has an ambitious plan to achieve 100 % renewable hydrogen targets by blending green hydrogen into the natural gas grid and evolving the grey hydrogen sector to blue with CCS technology by 2050 (Miller et al., 2020b). Canada has near-term plans to electrify the green hydrogen sector with nuclear and renewable sources with its abundant hydro energy sources and nuclear infrastructure with the potential to export green hydrogen to neighboring countries (Elmanakhly et al., 2021). Japan has a different strategy for increasing the efficiency of existing power plants and predicts to cover around 40 % of electrical energy demands with energy efficiency works in the sector. Other green hydrogen generation strategies include increasing RES share to 17 % by 2030, large hydrogen generation plants, and mini CHP applications for district heating and power (Iida and Sakata, 2019). China presently produces 30 % of all the Renewable energy globally and has plans to utilize renewable hydrogen for industry and residential sectors to decrease very high emission rates, as well as MW-scale CHP plants for district heating in certain regions to decrease natural gas-based emissions (Verheul, 2019; Ling et al., 2019). Hydrogen-related strategy documents have been published by many other governments, including many European countries, China, the US, Canada, Australia, the UK, Japan, South Korea, and New Zealand, while other strategy documents are on the way from governments that are agreed to the Paris Climate Change agreement. Many projected large-scale green hydrogen plants in various locations around the world are based on solar-electrolysis or wind-electrolysis coupling technologies. Table 5 has summarized more details of the prospective green hydrogen and ammonia plants worldwide.

Summary and conclusions

Clean hydrogen technologies have already taken their place in the energy industry ecosystem to meet hydrogen needs for the industry at a medium-scale level. A few large-scale plants are expected to be completed in the next decade to initiate a sustainable ecosystem era to help reduce GWP emissions from the industrial sector.

Despite ongoing research to enhance the operational and

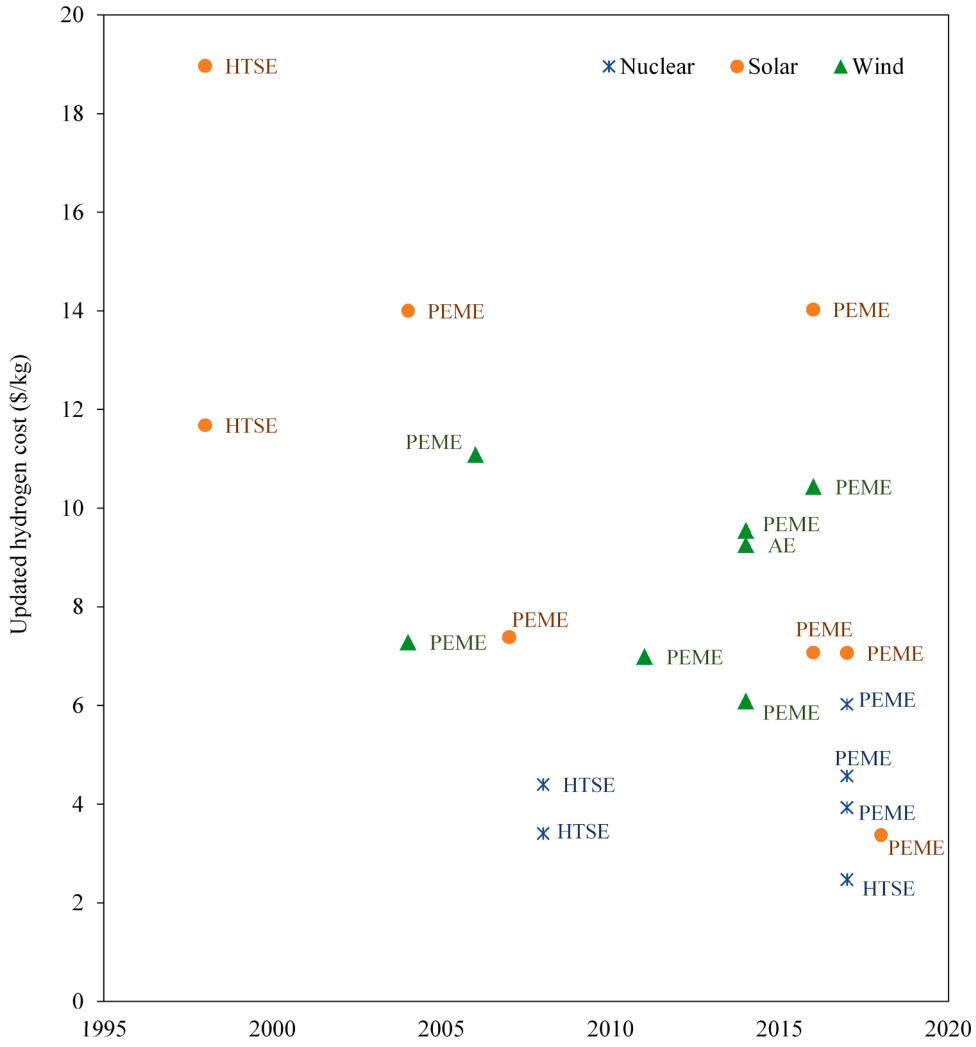


Fig. 7. Cost of hydrogen production using electrochemical water splitting driven by different clean energy sources (US dollar values are updated to 2022 with consideration of 2.5 % inflation) (El-Emam and Dincer, 2015; El-Emam and Dincer, 2014; El-Emam et al., 2014; El-Emam et al., 2015b; Amos, 2004; Choi et al., 2005b; Graf et al., 2008; Harvego et al., 2008; Gorensek et al., 2009; Bartels et al., 2010b; Lemus and Duart, 2010b; Kalinci et al., 2015; Abuşoğlu et al., 2016; El-Emam et al., 2016; Al-Sharafi et al., 2017; Boudries, 2018; El-Emam and Khamis, 2019).

performance characteristics of PEM and AE electrolyzers, these devices are already in the hydrogen market at a high technology readiness level.

After the Paris Climate Change Agreement, many countries have announced their national strategies and objectives for zero-emission targets by commissioning the protectional use of green hydrogen technologies. Many countries that signed the Paris Agreement have already published or announced their prospective visions and road-mapping documents to contribute towards decreasing emissions by launching near-to-long-term plans to invest massively in renewables and green hydrogen production development. An international collaborative ecosystem is essential to fulfilling the ambitious "net-zero" emission targets by 2050.

PEM and AE technologies have relatively high operational reliability and acceptable performance characteristics. Improving the electrochemical stability of the electrodes and enhancing the thermomechanical properties and ionic conductivity of the membrane, along with developing engineering and advanced materials for creating highly efficient stacks, will keep being the focus of the research advancement for manufacturing more durable and efficient electrolysis stacks in the short term. The SOEC and AEM electrolyzers still have a way to enter the hydrogen production market, which is expected to occur in the next decade. The SOEC technology, in particular, will need revolutionary solid-state Ionics to overcome the current challenges associated with its thermomechanical and thermochemical instability at high operating temperatures. Likewise, improving the durability of the AEM membrane will be central to increasing the market readiness level in the near term.

The anticipated green hydrogen plants will be developed mainly based on the PEM or AE technologies coupled with wind and/or solar PV power systems. The levelized cost of hydrogen is expected to be around USD 2–2.2 /kg H2 for large-scale plants in the near term, which will be comparable to that produced as grey hydrogen. However, the levelized cost of hydrogen is subject to change as a function of many variables, including the oil & gas price, carbon tax, and further fluctuations in the manufacturing costs of renewable harvesting devices and electrochemical cells.

The electrochemical hydrogen production based on renewables will flourish in the short term in various capacities and locations worldwide. Today, the largest PEM electrolyzer plant of around 20 MW produces about 8 tons of hydrogen daily. The manufacturing capacity of solar PV- or wind-PEM coupled will increase in the next few years as a result of multiple projects already commissioned worldwide to be deployed before e2030.

Hydrogen is expected to replace the domination of the fossil-fuel economy in many sectors worldwide in the next decades. Sophisticated know-how and revolutionary infrastructural changes will be required to deploy the hydrogen economy at a large scale. Further

Table 5
Projected green hydrogen and ammonia projects worldwide (Collins, 2021; Durakovic, 2021; Heartquist, 2021).

Project Name	Location	Power Source	Investment partners	Hydrogen production rate (million ton/y)	Purpose of use	Stage of development	Plant cost (USD)	Planned date of deployment
Shell	Germany	Wind (0.2 GW)	Shell, Refhyne consortium	0.013	Refineries	Operating	Not stated	2021
SGH2	USA	Paper waste	SGH2	0.004	Various at USD 2/ kg cost	Commissioning	Not stated	2023
HyDeal	Western Europe	Solar PV (95 GW)	Energas,OGE, McPhy, Qair	3.6 (Total for various plants)	Delivery of green hydrogen across EU	Early stage	Not stated	2030
Western Green Energy Hub	Australia	Solar –wind (50 GW)	Intercontinental, CWP global	3.5 H_2 or 20 NH_3	For export or local use	Very early stage	~70 bn	After 2028
Unnamed	Kazakhstan	Solar-wind (45 GW)	Svevnin Energy, Kazakh Investment agency	~ 3	For export or local use	Very early stage	Not stated	After 2027
Aman	Mauritania	Wind-solar (30 GW)	CWP Global – Mauritania Authorities,	Not stated	Green steel making, long distance shipping	Very early stage	Not stated	Not Stated (Agreement signed on 2021)
Unnamed	Oman	Wind and solar (25 GW)	InerContinental energy, Omani oil, enerTEch	Not stated	Sales on international markets	Early stage	~ 10 bn	After 2028
Asian RE	Australia	Onshore Wind (10 GW) solar (14 GW)	CWP Asia, InterContinental, Vestas, Macquarie	1.75 (9.9 NH_3)	Hydrogen ammonia exports to Asian markets	Discussion between government-stakeholders	~70 bn	2027–2028
NortH2	Netherlands	Off-shore wind (>10 GW)	Shell, Equinor, RWE, GAsunie, Groningen Seaports	1	Powering heavy industries	Feasibility studies underway	Not stated	1 GW by 2027 4 GW by 2030 Completion by 2040
Aqua Ventus	Germany	Off-shore wind (10 GW)	47 companies including Shell, RWE, Siemens	1	EU hydrogen network	Early stage	Not stated	30 MW by 2025 5 GW by 2030 Completion by 2035
Hyenergy	Australia	Wind and solar (8 GW)	Provincial investment	Not stated	Hydrogen ammonia exports to Asian markets	Early stage	Not stated	2030
Murchison	Australia	Onshore wind – solar (5 GW)	Hydrogen Renewables Australia, Copenhagen Infrastructure	Not stated	Hydrogen to blend into NG pipelines, export	Early stage	10–12 bn	2028
Beijing Jingneng	China	Onshore wind-solar	Chine's Utility Beijing Jingneng	0.4–0.5	Not stated	Construction started in 2021	3 bn	After 2021
Helios Green Fuels	Saudi Arabia	Onshore wind –solar (4 GW)	Air Products, ACWA power, Neom	0.24 (1.2 NH_3)	Green ammonia, transport fuel	Early stage	5 bn	2025
Pacific	Australia	Solar (3.6GW)	Austrom Hydrogen	0.2	Export to international markets	Early stage	Not stated	Not stated
Base One	Brazil	Wind-solar (3.4 GW)	Enegix energy, Enerwind, Black&Veatch	0.6	Export to international markets	Contracted	5.4 bn	2025
Southwest Ireland	Ireland	Offshore wind (3.2 GW)	Zenith Energy, US oil & gas company, EI-H2	Not stated	Green Ammonia	Very early stage	Not stated	2028
H2-Hub	Australia	RES (3 GW)	H2U	1.8 NH_3	Green Ammonia	Early stage	1.6 bn	2025
Yellow Sea	China	Floating Wind (2GW)	Power China Northwest Engineering Institute	Not stated	Not stated	Very early stage	Not stated	Not stated
Green H2 & Chemicals	Oman	Wind-solar (2 GW)	Indian ACME	0.146	Green Ammonia	Under development	3.3 bn	2022
HyEx	Chile	Solar (1.6 GW)	Engie, Enaex	0.124	Green Ammonia, export	Early stage	Not stated	26 MW pilot plant by 2024 Completion by 2030
White Dragon	Greece	Soalr (1.5 GW)	Public Authorities, and private investors	0.25	Baseload power via FC, export,	Plan submitted to EU and public authorities	8 bn	2029
Geraldton	Australia	Onshore wind – solar (1.5 GW)	BP	Not stated	Green ammonia for domestic use and export	Feasibility study	Not stated	Not stated
HNH	Chile	Onshore Wind (1.8 GW)	AustriaEnergy. Okowind EE	0.85	Green ammonia for export	Design stage	3 bn	2026
Greater Copenhagen	Denmark	Offshore wind (1.3 GW)	Orsted, Maersk, DSV Panalpia, DFDS, SAS	0.25 (synthetic fuel)	Energy for transportation	Feasibility study	Not stated	10 MW pilot plant by 2023 Completion 2030

(*continued on next page*)

Table 5 (*continued*)

Project Name	Location	Power Source	Investment partners	Hydrogen production rate (million ton/y)	Purpose of use	Stage of development	Plant cost (USD)	Planned date of deployment
seaH2land	Netherlands, Belgium	Offshore wind (2 GW)	Orsted, ArcelorMittal, Yara, Dow Benelux, Zeeland	Not stated	Industrial clusters	Early stage	Not stated	2030
Esbjerg	Denmark	Offshore wind (1 GW)	Moller-Maersk, DFDS, Arla, DLG	Not stated	Green ammonia	Early stage	Not stated	2027
H2 Sines	Denmark	Not decided (1 GW)	EDP, Galp, Martifier, REN, Vestas	Not stated	Domestic consumption, export	Early stage	1.8 bn	2030
Rostock	Germany	Offshore wind and other RES (1 GW)	RWE	Not stated	Not stated	Very early stage	Not stated	Not stated

research studies and deployment investigation are an essential part of this journey to gain more knowledge about hydrogen production, storage, and utilization before such a massive change. Therefore, many national and international initiatives are acting accordingly to lead the world hydrogen market in the era of "net-zero" emissions.

Declaration of Competing Interest

The authors declare that they have no known competing financial interests or personal relationships that could have appeared to influence the work reported in this paper.

Acknowledgments

The corresponding author thanks the Royal Academy of Engineering for the Leverhulme Trust Research Fellowship (LTRF2021\17131) for financial support. The authors also thank the Technology Transfer Office at the University of Surrey, particularly Dr William Mortimore and Dr William Lovegrove, for their tremendous support for this project.

References

Abuşoğlu, A., Demir, S., Özahi, E., 2016. Energy and economic analyses of models developed for sustainable hydrogen production from biogas-based electricity and sewage sludge. Int. J. Hydrogen Energy 41 (31).
Acar, C., et al., 2019. Transition to a new era with light-based hydrogen production for a carbon-free society: an overview. Int. J. Hydrogen Energy 44 (47), 25347–25364.
Acar, C., Dincer, I., 2014. Comparative assessment of hydrogen production methods from renewable and non-renewable sources. Int. J. Hydrogen Energy 39 (1), 1–12.
Ahn, S.H., et al., 2013. Electrochemically fabricated NiCu alloy catalysts for hydrogen production in alkaline water electrolysis. Int. J. Hydrogen Energy 38 (31), 13493–13501.
Ahn, S.H., et al., 2014. Development of a membrane electrode assembly for alkaline water electrolysis by direct electrodeposition of nickel on carbon papers. Appl. Catal. B 154, 197–205.
Ahn, S.H., et al., 2016. Anion exchange membrane water electrolyzer with an ultra-low loading of Pt-decorated Ni electrocatalyst. Appl. Catal. B 180, 674–679.
Aicart, J., et al., 2022. Performance evaluation of a 4-stack solid oxide module in electrolysis mode. Int. J. Hydrogen Energy 47 (6), 3568–3579.
Aili, D., et al., 2015. Porous poly(perfluorosulfonic acid) membranes for alkaline water electrolysis. J. Memb. Sci. 493, 589–598.
Alavi, O., Mostafaeipour, A., Qolipour, M., 2016. Analysis of hydrogen production from wind energy in the southeast of Iran. Int. J. Hydrogen Energy 41 (34), 15158–15171.
Allebrod, F., Chatzichristodoulou, C., Mogensen, M.B., 2013. Alkaline electrolysis cell at high temperature and pressure of 250 °C and 42 bar. J. Power Sources 229, 22–31.
Allebrod, F., Chatzichristodoulou, C., Mogensen, M.B., 2014. Cobalt and molybdenum activated electrodes in foam based alkaline electrolysis cells at 150–250 °C and 40 bar. J. Power Sources 255, 394–403.
Al-Qahtani, A., et al., 2021. Uncovering the true cost of hydrogen production routes using life cycle monetisation. Appl. Energy 281, 115958.
Al-Sharafi, A., et al., 2017. Techno-economic analysis and optimization of solar and wind energy systems for power generation and hydrogen production in Saudi Arabia. Renew. Sustainab. Energy Rev. 69.
AlZahrani, A., *Investigation of a novel high temperature solid oxide electrolyzer for solar hydrogen production.* 2017.
AlZahrani, A.A., Dincer, I., 2016. Design and analysis of a solar tower based integrated system using high temperature electrolyzer for hydrogen production. Int. J. Hydrogen Energy 41 (19), 8042–8056.
Amikam, G., Nativ, P., Gendel, Y., 2018. Chlorine-free alkaline seawater electrolysis for hydrogen production. Int. J. Hydrogen Energy 43 (13), 6504–6514.
Amos, W.A., 2004. Updated Cost Analysis of Photobiological Hydrogen Production from Chlamydomonas Reinhardtii Green Algae: Milestone Completion Report. National Renewable Energy Lab, Golden, COUS.
Antonucci, V., et al., 2008. High temperature operation of a composite membrane-based solid polymer electrolyte water electrolyser. Electrochim. Acta 53 (24), 7350–7356.
Awasthi, A., Scott, K., Basu, S., 2011. Dynamic modeling and simulation of a proton exchange membrane electrolyzer for hydrogen production. Int. J. Hydrogen Energy 36 (22), 14779–14786.
Ayers, K., 2021. High efficiency PEM water electrolysis: enabled by advanced catalysts, membranes, and processes. Curr. Opin. Chem. Eng. 33, 100719.
Baglio, V., et al., 2009. Solid polymer electrolyte water electrolyser based on nafion-TiO2 composite membrane for high temperature operation. Fuel Cell. 9 (3), 247–252.
Balta, M.T., Dincer, I., Hepbasli, A., 2009. Thermodynamic assessment of geothermal energy use in hydrogen production. Int. J. Hydrogen Energy 34 (7), 2925–2939.
Bamisile, O., et al., 2020. Environmental impact of hydrogen production from Southwest China's hydro power water abandonment control. Int. J. Hydrogen Energy 45 (46), 25587–25598.
Baran, E., et al., 2017. TiO2-NT electrodes modified with Ag and diamond like carbon (DLC) for hydrogen production by alkaline water electrolysis. Appl. Surf. Sci. 420, 416–428.
Barbir, F., 2005. PEM electrolysis for production of hydrogen from renewable energy sources. Sol. Energy 78 (5), 661–669.
Bartels, J.R., Pate, M.B., Olson, N.K., 2010b. An economic survey of hydrogen production from conventional and alternative energy sources. Int. J. Hydrogen Energy 35 (16).
Bartels, J.R., Pate, M.B., Olson, N.K., 2010a. An economic survey of hydrogen production from conventional and alternative energy sources. Int. J. Hydrogen Energy 35 (16), 8371–8384.
Bernadet, L., et al., 2020. High-performing electrolyte-supported symmetrical solid oxide electrolysis cells operating under steam electrolysis and co-electrolysis modes. Int. J. Hydrogen Energy 45 (28), 14208–14217.
Bhandari, R., Trudewind, C.A., Zapp, P., 2014. Life cycle assessment of hydrogen production via electrolysis–a review. J. Clean. Prod. 85, 151–163.
Bianco, E., Blanco, H., 2020. Green Hydrogen: a Guide to Policy Making.
Birol, F., 2019b. The Future of Hydrogen (IEA). Paris.
Birol, F., 2019a. Report prepared by the IEA for the G20, pp. 82–83. Japan.
Blanco, H., et al., 2018. Potential for hydrogen and Power-to-Liquid in a low-carbon EU energy system using cost optimization. Appl. Energy 232, 617–639.
Bo, Y., et al., 2010. Status and research of highly efficient hydrogen production through high temperature steam electrolysis at INET. Int. J. Hydrogen Energy 35 (7), 2829–2835.
Bockris, J.O.M., et al., 1980. Comprehensive Treatise of Electrochemistry, 1. Springer.
Bødal, E.F., Korpås, M., 2020. Value of hydro power flexibility for hydrogen production in constrained transmission grids. Int. J. Hydrogen Energy 45 (2), 1255–1266.
Böhm, D., et al., 2021. Highly conductive titania supported iridium oxide nanoparticles with low overall iridium density as OER catalyst for large-scale PEM electrolysis. Applied Materials Today 24, 101134.
Bolobov, V., 2002. Mechanism of self-ignition of titanium alloys in oxygen. Combust. Explos. Shock Wave. 38 (6), 639–645.
Boudries, R., 2018. Techno-economic study of hydrogen production using CSP technology. Int. J. Hydrogen Energy 43 (6).
Briant, C., Wang, Z., Chollocoop, N., 2002. Hydrogen embrittlement of commercial purity titanium. Corros. Sci. 44 (8), 1875–1888.
Burhan, M., et al., 2017. Solar to hydrogen: compact and cost effective CPV field for rooftop operation and hydrogen production. Appl. Energy 194, 255–266.
Cai, Q., Brandon, N.P., Adjiman, C.S., 2010. Modelling the dynamic response of a solid oxide steam electrolyser to transient inputs during renewable hydrogen production. Front. Energy Power Eng. Chin. 4 (2), 211–222.
Carmo, M., et al., 2013. A comprehensive review on PEM water electrolysis. Int. J. Hydrogen Energy 38 (12), 4901–4934.
Cetinkaya, E., Dincer, I., Naterer, G., 2012. Life cycle assessment of various hydrogen production methods. Int. J. Hydrogen Energy 37 (3), 2071–2080.
Chanda, D., et al., 2014. Evolution of physicochemical and electrocatalytic properties of NiCo2O4 (AB2O4) spinel oxide with the effect of Fe substitution at the A site leading

to efficient anodic O2 evolution in an alkaline environment. Int. J. Hydrogen Energy 39 (11), 5713–5722.
Chanda, D., et al., 2017. Optimization of synthesis of the nickel-cobalt oxide based anode electrocatalyst and of the related membrane-electrode assembly for alkaline water electrolysis. J. Power Source. 347, 247–258.
Chandesris, M., et al., 2015. Membrane degradation in PEM water electrolyzer: numerical modeling and experimental evidence of the influence of temperature and current density. Int. J. Hydrogen Energy 40 (3), 1353–1366.
Chen, K., 2016. Materials degradation of solid oxide electrolysis cells. J. Electrochem. Soc. 163 (11), F3070.
Chen, P., Hu, X., 2020. High-efficiency anion exchange membrane water electrolysis employing non-noble metal catalysts. Adv. Energy Mater. 10 (39), 2002285.
Cheng, J., et al., 2009b. Preparation of Ir0.4Ru0.6MoxOy for oxygen evolution by modified Adams' fusion method. Int. J. Hydrogen Energy 34 (16), 6609–6613.
Cheng, J., et al., 2009a. Study of IrxRu1-xO2 oxides as anodic electrocatalysts for solid polymer electrolyte water electrolysis. Electrochim. Acta 54 (26), 6250–6256.
Cherevko, S., et al., 2016. Oxygen and hydrogen evolution reactions on Ru, RuO_2, Ir, and IrO_2 thin film electrodes in acidic and alkaline electrolytes: a comparative study on activity and stability. Catal. Today 262, 170–180.
Chisholm, G., Cronin, L., 2016. *Hydrogen from Water electrolysis*, in *Storing Energy*. Elsevier, pp. 315–343.
Cho, M.K., et al., 2018. Alkaline anion exchange membrane water electrolysis: effects of electrolyte feed method and electrode binder content. J. Power Sources 382, 22–29.
Choi, J.H., et al., 2005b. Hydrogen production costs of various primary energy sources. In: Korean Nuclear Society Conference. Korean Nuclear Society.
Choi, J.H., et al., *Hydrogen production costs of various primary energy sources.* 2005.
Christopher, K., Dimitrios, R., 2012. A review on exergy comparison of hydrogen production methods from renewable energy sources. Energy Environ. Sci. 5 (5), 6640–6651.
Collins, L., 2021. Global Green-Hydrogen Pipeline Exceeds 250GW — Here's the 27 Largest Gigawatt-Scale Projects [cited 2021 29/10/2021]; Available from: https://www.rechargenews.com/energy-transition/global-green-hydrogen-pipeline-exceeds-250gw-heres-the-27-largest-gigawatt-scale-projects/2-1-933755.
Commission, E.E., 2018. *A Clean Planet for all–A European long-term strategic vision for a prosperous, modern, competitive and climate neutral economy*. depth analysis in support of the commission. Commun. COM (2018) 773, 2018.
Corrales-Sánchez, T., Ampurdanés, J., Urakawa, A., 2014. MoS2-based materials as alternative cathode catalyst for PEM electrolysis. Int. J. Hydrogen Energy 39 (35), 20837–20843.
Cossar, E., et al., 2019. The performance of nickel and nickel-iron catalysts evaluated as anodes in anion exchange membrane water electrolysis. Catalysts 9 (10), 814.
Cossar, E., et al., 2021. Ionomer content optimization in nickel-iron-based anodes with and without ceria for anion exchange membrane water electrolysis. J. Power Sources 514, 230563.
Council, H., *Hydrogen Scaling up: a Sustainable Pathway for the Global Energy Transition.* 2017.
Council, H., *Path to hydrogen competitiveness: a cost perspective.* 2020.
Council, N.R., 2004. The Hydrogen economy: opportunities, costs, barriers, and R&D Needs. National Academies Press.
David, M., Ocampo-Martínez, C., Sánchez-Peña, R., 2019. Advances in alkaline water electrolyzers: a review. J. Energy Storage 23, 392–403.
Debe, M., et al., 2012. Initial performance and durability of ultra-low loaded NSTF electrodes for PEM electrolyzers. J. Electrochem. Soc. 159 (6), K165.
Department for Business, E.a.I.S.B, 2016. Electricity Generation Costs.
Devarayapalli, K.C., et al., 2022. Nanostructured cobalt-based metal-organic framework/cadmium sulfide electrocatalyst for enhanced oxygen evolution reaction and anion exchange membrane-based water electrolysis: synergistic effect. J. Power Sources 527, 231151.
Diaz, L.A., et al., 2016. Alkali doped poly (2,5-benzimidazole) membrane for alkaline water electrolysis: characterization and performance. J. Power Sources 312, 128–136.
Di Blasi, A., et al., 2013. Evaluation of materials and components degradation of a PEM electrolyzer for marine applications. Int. J. Hydrogen Energy 38 (18), 7612–7615.
Di Dio, V., et al., 2009. The use of sea waves for generation of electrical energy and hydrogen. OCEANS 2009. IEEE.
Dincer, I., Acar, C., 2015. Review and evaluation of hydrogen production methods for better sustainability. Int. J. Hydrogen Energy 40 (34), 11094–11111.
Dincer, I. and H. Ozcan, *1.17 Geothermal Energy*. 2018.
DiPippo, R., 2016. Geothermal Power generation: Developments and Innovation. Woodhead Publishing.
Doan, T.L., et al., 2022. Influence of IrO2/TiO2 coated titanium porous transport layer on the performance of PEM water electrolysis. J. Power Sources 533, 231370.
Dönitz, W., Erdle, E., 1985. High-temperature electrolysis of water vapor—Status of development and perspectives for application. Int. J. Hydrogen Energy 10 (5), 291–295.
Drive, U., 2017. Hydrogen Production Tech Team Roadmap, 2. US Department of Energy. Retrieved, p. 2019.
Durakovic, A., 2021. Shell Starts Up Green Hydrogen Electrolyser at German Refinery [cited 2021 29/10/2021]; Available from: https://www.offshorewind.biz/2021/07/05/shell-starts-up-green-hydrogen-electrolyser-at-german-refinery/.
Egelund, S., et al., 2016. Manufacturing of a LaNiO3 composite electrode for oxygen evolution in commercial alkaline water electrolysis. Int. J. Hydrogen Energy 41 (24), 10152–10160.
El-Emam, R., Khamis, I., 2017. International collaboration in the IAEA nuclear hydrogen production program for benchmarking of HEEP. Int. J. Hydrogen Energy 42 (6), 3566–3571.
El-Emam, R., Khamis, I., 2019. Recent advances in Nuclear Hydrogen Production: results from IAEA Coordinated Research Project. Int. J. Hydrogen Energy 44 (35).
El-Emam, R.S., Bhattacharyya, R., 2021. Toward the deployment of nuclear cogeneration projects–issues and considerations. Energy Sources Part A 1–14.
El-Emam, R.S., Dincer, I., 2014. Comparative study on nuclear based hydrogen production: cost assessment. In: International Conference on Smart Energy Grid Engineering (SEGE). University of Ontario Institute of Technology, Oshawa, ON, Canada.
e.a. El-Emam, R.S., Dincer, I., 2015. Hydrogen production from nuclear energy: comparative cost assessment. In: Dincer, I. (Ed.), Progress in Clean Energy Vol. II: Novel Systems and Applications. Springer. e.a.Editor.
El-Emam, R.S., Dincer, I., 2018. Nuclear-Assisted Hydrogen Production.
El-Emam, R.S., Gabriel, K.S., 2021. Synergizing hydrogen and cement industries for Canada's climate plan – case study. Energy Source. Part A 43 (23), 3151–3165.
El-Emam, R.S., I. Khamis, and I. Dincer, *Economic assessment of the Cu-Cl thermochemical cycle coupled with SCWR for large scale hydrogen production*, in *4th IEEE International Conference on Smart Energy Grid Engineering*. 2016: Oshawa, ON, Canada.
El-Emam, R.S., Özcan, H., 2019. Comprehensive review on the techno-economics of sustainable large-scale clean hydrogen production. J. Clean. Prod. 220, 593–609.
El-Emam, R.S., H. Ozcan, and I. Dincer, *Cost assessment of nuclear hydrogen production systems using HEEP*, in *7th International Ege Energy Symposium & Exhibition (IEESE)*. 2014: Usak, Turkey.
El-Emam, R.S., Ozcan, H., Dincer, I., 2015b. Comparative cost evaluation of nuclear hydrogen production methods with the Hydrogen Economy Evaluation Program (HEEP). Int. J. Hydrogen Energy 40 (34).
El-Emam, R.S., Ozcan, H., Dincer, I., 2015a. Comparative cost evaluation of nuclear hydrogen production methods with the Hydrogen Economy Evaluation Program (HEEP). Int. J. Hydrogen Energy 40 (34), 11168–11177.
El-Emam, R.S., Zamfirescu, C., Gabriel, K.S., 2023. Chapter 19 - Hydrogen production pathways for Generation-IV reactors. In: Pioro, I.L. (Ed.), Handbook of Generation IV Nuclear Reactors, 2nd Edition. Woodhead Publishing, pp. 665–680. Editor.
Elmanakhly, F., et al., 2021. Hydrogen economy transition plan: a case study on Ontario. AIMS Energy 9 (4), 775–811.
Erdle, E., et al., 1992. Reversibility and polarization behaviour of high temperature solid oxide electrochemical cells. Int. J. Hydrogen Energy 17 (10), 817–819.
Evans, A., Strezov, V., Evans, T.J., 2009. Assessment of sustainability indicators for renewable energy technologies. Renew. Sustainab. Energy Rev. 13 (5), 1082–1088.
Ewing, M., et al., 2020. Hydrogen on the Path to Net-Zero Emissions.
Faid, A.Y., et al., 2018. Highly active nickel-based catalyst for hydrogen evolution in anion exchange membrane electrolysis. Catalysts 8 (12), 614.
Faid, A.Y., et al., 2021. NiCu mixed metal oxide catalyst for alkaline hydrogen evolution in anion exchange membrane water electrolysis. Electrochim. Acta 371, 137837.
Faid, A.Y., et al., 2022. Ternary NiCoFe nanosheets for oxygen evolution in anion exchange membrane water electrolysis. Int. J. Hydrogen Energy 47 (56), 23483–23497.
Faisal, N.H., et al., 2022. Application of thermal spray coatings in electrolysers for hydrogen production: advances, challenges, and opportunities. ChemNanoMat, e202200384.
Falcão, D., Pinto, A., 2020. A review on PEM electrolyzer modelling: guidelines for beginners. J. Clean. Prod. 261, 121184.
Fallah Vostakola, M., et al., 2023. Recent advances in high-temperature steam electrolysis with solid oxide electrolysers for green hydrogen production. Energies 16 (8), 3327.
Fallah Vostakola, M., Horri, B.A., 2021. Progress in material development for low-temperature solid oxide fuel cells: a review. Energies 14 (5), 1280.
Fallah Vostakola, M., Salamatinia, B., Amini Horri, B., 2022. A review on recent progress in the integrated green hydrogen production processes. Energies 15 (3), 1209.
Fang, Q., Packbier, U., Blum, L., 2013. Long-term tests of a Jülich planar short stack with reversible solid oxide cells in both fuel cell and electrolysis modes. Int. J. Hydrogen Energy 38 (11), 4281–4290.
Feng, Q., et al., 2017. A review of proton exchange membrane water electrolysis on degradation mechanisms and mitigation strategies. J. Power Source. 366, 33–55.
Ferrero, D., et al., 2013. A comparative assessment on hydrogen production from low- and high-temperature electrolysis. Int. J. Hydrogen Energy 38 (9), 3523–3536.
Fortin, P., et al., 2020. High-performance alkaline water electrolysis using Aemion™ anion exchange membranes. J. Power Source. 451, 227814.
Frensch, S.H., et al., 2019. Influence of the operation mode on PEM water electrolysis degradation. Int. J. Hydrogen Energy 44 (57), 29889–29898.
Fujishima, A., Honda, K., 1972. Electrochemical photolysis of water at a semiconductor electrode. Nature 238 (5358), 37–38.
Gabriel, K.S., El-Emam, R.S., Zamfirescu, C., 2022. Technoeconomics of large-scale clean hydrogen production – a review. Int. J. Hydrogen Energy 47 (72), 30788–30798.
Gago, A., et al., 2016. Protective coatings on stainless steel bipolar plates for proton exchange membrane (PEM) electrolysers. J. Power Sources 307, 815–825.
Ganley, J.C., 2009. High temperature and pressure alkaline electrolysis. Int. J. Hydrogen Energy 34 (9), 3604–3611.
García-Valverde, R., Espinosa, N., Urbina, A., 2012. Simple PEM water electrolyser model and experimental validation. Int. J. Hydrogen Energy 37 (2), 1927–1938.
Ghazvini, M., et al., 2019. Geothermal energy use in hydrogen production: a review. Int. J. Energy Res. 43 (14), 7823–7851.
Goñi-Urtiaga, A., Presvytes, D., Scott, K., 2012. Solid acids as electrolyte materials for proton exchange membrane (PEM) electrolysis. Int. J. Hydrogen Energy 37 (4), 3358–3372.
Gorensek, M., et al., 2009. Hybrid Sulfur Process Reference Design and Cost Analysis. United Statesp. Medium: ED.

Graf, D., et al., 2008. Economic comparison of solar hydrogen generation by means of thermochemical cycles and electrolysis. Int. J. Hydrogen Energy 33 (17).
Greiner, C.J., KorpÅs, M., Holen, A.T., 2007. A Norwegian case study on the production of hydrogen from wind power. Int. J. Hydrogen Energy 32 (10–11), 1500–1507.
Grigor'ev, S.A., et al., 2001. Electrolysis of water in a system with a solid polymer electrolyte at elevated pressure. Elektrokhimiya 37 (8), 953–958.
Grigoriev, S.A., et al., 2009b. Optimization of porous current collectors for PEM water electrolysers. Int. J. Hydrogen Energy 34 (11), 4968–4973.
Grigoriev, S.A., et al., 2009a. Hydrogen safety aspects related to high-pressure polymer electrolyte membrane water electrolysis. Int. J. Hydrogen Energy 34 (14), 5986–5991.
Grigoriev, S.A., et al., 2014. Failure of PEM water electrolysis cells: case study involving anode dissolution and membrane thinning. Int. J. Hydrogen Energy 39 (35), 20440–20446.
Grigoriev, S.A., Millet, P., Fateev, V.N., 2008. Evaluation of carbon-supported Pt and Pd nanoparticles for the hydrogen evolution reaction in PEM water electrolysers. J. Power Source. 177 (2), 281–285.
Guban, D., et al., 2020. Assessment of sustainable high temperature hydrogen production technologies. Int. J. Hydrogen Energy 45 (49), 26156–26165.
Guo, W., et al., 2022. Electrochemically activated Ni@Ni(OH)2 heterostructure as efficient hydrogen evolution reaction electrocatalyst for anion exchange membrane water electrolysis. Mater. Today Chem. 24, 100994.
Guoqiang, W., et al., 2010. SPE water electrolysis with SPEEK/PES blend membrane. Int. J. Hydrogen Energy 35 (15), 7778–7783.
Harvego, E.A., et al., 2008. Economic Analysis of the Reference Design for a Nuclear-Driven High-Temperature-Electrolysis Hydrogen Production Plant. Idaho National Laboratory (INL).
Hauch, A., et al., 2008. Solid oxide electrolysis cells: microstructure and degradation of the Ni/yttria-stabilized zirconia electrode. J. Electrochem. Soc. 155 (11), B1184.
Hausfather, Z., Peters, G.P., 2020. Emissions–the 'business as Usual'story is Misleading. Nature Publishing Group.
He, W., et al., 2020. Thermodynamic analysis of a solar-driven high-temperature steam electrolyzer for clean hydrogen production. Appl. Therm. Eng. 172, 115152.
Heartquist, C., 2021. World's Largest Green Hydrogen Project to Launch in California [cited 2021 29/10/2021]; Available from: https://www.sgh2energy.com/worlds-largest-green-hydrogen-project-to-launch-in-california.
Henkensmeier, D., et al., 2021. Overview: state-of-the art commercial membranes for anion exchange membrane water electrolysis. J. Electrochem. Energy Convers. Storage 18 (2), 024001.
Hinkley, J., et al., 2016. Report to ARENA as part of Solar Fuels Roadmap, Project A-3018, pp. 1–4.
Ho, T.X., et al., 2009. Modeling of transport, chemical and electrochemical phenomena in a cathode-supported SOFC. Chem. Eng. Sci. 64 (12), 3000–3009.
Horri, B.A., et al., 2019. A highly efficient hydrogen generation electrolysis system using alkaline zinc hydroxide solution. Int. J. Hydrogen Energy 44 (1), 72–81.
Horri, B.A., Selomulya, C., Wang, H., 2012. Electrochemical characteristics and performance of anode-supported SOFCs fabricated using carbon microspheres as a pore-former. Int. J. Hydrogen Energy 37 (24), 19045–19054.
Hou, S., Xie, K., 2019. Enhancing the performance of high-temperature H2O/CO2 co-electrolysis process on the solid oxide Sr2Fe1.6Mo0.5O6-δ-SDC/LSGM/Sr2Fe1.5Mo0.5O6-δ-SDC cell. Electrochim. Acta 301, 63–68.
Hu, G., et al., 2020. A review of technical advances, barriers, and solutions in the power to hydrogen (P2H) roadmap. Engineering.
Huang, K., et al., 1996. Characterization of Sr-Doped LaMnO3 and LaCoO3 as cathode materials for a doped $LaGaO_3$ ceramic fuel cell. J. Electrochem. Soc. 143 (11), 3630.
Huang, M., et al., 2022. LSCM-GDC as composite cathodes for high temperature steam electrolysis: performance optimization by composition and microstructure tailoring. Int. J. Hydrogen Energy 47 (82), 34784–34793.
Hung, Y., El-Khatib, K., Tawfik, H., 2005. Corrosion-resistant lightweight metallic bipolar plates for PEM fuel cells. J. Appl. Electrochem. 35 (5), 445–447.
Iida, S., Sakata, K., 2019. Hydrogen technologies and developments in Japan. Clean Energy 3 (2), 105–113.
Ioroi, T., et al., 2002. Thin film electrocatalyst layer for unitized regenerative polymer electrolyte fuel cells. J. Power Source. 112 (2), 583–587.
Ishaq, H., Dincer, I., 2020. Performance investigation of adding clean hydrogen to natural gas for better sustainability. J. Nat. Gas Sci. Eng. 78, 103236.
Ishaq, H., Dincer, I., Naterer, G.F., 2018. Performance investigation of an integrated wind energy system for co-generation of power and hydrogen. Int. J. Hydrogen Energy 43 (19), 9153–9164.
Ito, H., et al., 2018. Experimental investigation of electrolytic solution for anion exchange membrane water electrolysis. Int. J. Hydrogen Energy 43 (36), 17030–17039.
James, B.D., DeSantis, D.A., Saur, G., 2016. Hydrogen Production Pathways Cost Analysis (2013–2016). Strategic Analysis Inc., Arlington, VAUnited States.
Jang, M.J., et al., 2020. Superior performance and stability of anion exchange membrane water electrolysis: pH-controlled copper cobalt oxide nanoparticles for the oxygen evolution reaction. J. Mater. Chem. A 8 (8), 4290–4299.
Jiang, W., et al., 2022. Composition-Dependent Morphology, Structure, and Catalytical Performance of Nickel–Iron Layered Double Hydroxide as Highly-Efficient and Stable Anode Catalyst in Anion Exchange Membrane Water Electrolysis. Adv. Funct. Mater. 32 (38), 2203520.
Jones, R.H., Thomas, G.J., 2007. Materials For the Hydrogen Economy. CRC Press.
Kadakia, K.S., et al., 2014. Nanostructured F doped IrO2 electro-catalyst powders for PEM based water electrolysis. J. Power Source. 269, 855–865.
Kaleibari, S.S., Yanping, Z., Abanades, S., 2019. Solar-driven high temperature hydrogen production via integrated spectrally split concentrated photovoltaics (SSCPV) and solar power tower. Int. J. Hydrogen Energy 44 (5), 2519–2532.
Kalinci, Y., Hepbasli, A., Dincer, I., 2015. Techno-economic analysis of a stand-alone hybrid renewable energy system with hydrogen production and storage options. Int. J. Hydrogen Energy 40 (24).
Kang, S.Y., et al., 2022. High-performance and durable water electrolysis using a highly conductive and stable anion-exchange membrane. Int. J. Hydrogen Energy 47 (15), 9115–9126.
Kato, Y., et al., 1997. Utilization of high temperature heat using a calcium oxide/lead oxide/carbon dioxide chemical heat pump. J. Chem. Eng. Jpn. 30 (6), 1013–1019.
Kato, Y., Harada, N., Yoshizawa, Y., 1999. Kinetic feasibility of a chemical heat pump for heat utilization of high-temperature processes. Appl. Therm. Eng. 19 (3), 239–254.
Khamis, I., 2011. An overview of the IAEA HEEP software and international programmes on hydrogen production using nuclear energy. Int. J. Hydrogen Energy 36 (6), 4125–4129.
Khan, M.S., et al., 2020. New insights into the degradation behavior of air electrodes during solid oxide electrolysis and reversible solid oxide cell operation. Energy Technology 8 (9), 2000241.
Khatib, F., et al., 2019. Material degradation of components in polymer electrolyte membrane (PEM) electrolytic cell and mitigation mechanisms: a review. Renew. Sustainab. Energy Rev. 111, 1–14.
Khelfaoui, N., et al., 2021. Experimental investigation of solar hydrogen production PV/PEM electrolyser performance in the Algerian Sahara regions. Int. J. Hydrogen Energy 46 (59), 30524–30538.
Kiebach, R., et al., 2017. A novel SOFC/SOEC sealing glass with a low SiO2 content and a high thermal expansion coefficient. ECS Trans. 78 (1), 1739.
Kim, J.H., et al., 2015. Low-cost and energy-efficient asymmetric nickel electrode for alkaline water electrolysis. Int. J. Hydrogen Energy 40 (34), 10720–10725.
Knobloch, F., et al., 2019. Simulating the deep decarbonisation of residential heating for limiting global warming to 1.5 C. Energ. Effic. 12 (2), 521–550.
Kokoh, K.B., et al., 2014. Efficient multi-metallic anode catalysts in a PEM water electrolyzer. Int. J. Hydrogen Energy 39 (5), 1924–1931.
Kondoh, M., et al., 2000. Development of solid polymer-electrolyte water electrolyser. J. New Mater. Electrochem. Syst. 3 (1), 61–65.
Kuleshov, N.V., et al., 2019. Development and performances of a 0.5 kW high-pressure alkaline water electrolyser. Int. J. Hydrogen Energy 44 (56), 29441–29449.
Kuleshov, V.N., et al., 2016. Development and characterization of new nickel coatings for application in alkaline water electrolysis. Int. J. Hydrogen Energy 41 (1), 36–45.
Kumar, S.S., et al., 2016. Hydrothermal assisted morphology designed MoS2 material as alternative cathode catalyst for PEM electrolyser application. Int. J. Hydrogen Energy 41 (31), 13331–13340.
Kumar, S.S., Himabindu, V., 2019. Hydrogen production by PEM water electrolysis–A review. Mater. Sci. Energy Technolog. 2 (3), 442–454.
LaConti, A., Swette, L., 2010. Special applications using PEM-technology. Handbook of Fuel Cells.
Lædre, S., et al., 2017. Materials for proton exchange membrane water electrolyzer bipolar plates. Int. J. Hydrogen Energy 42 (5), 2713–2723.
Laguna-Bercero, M., 2012. Recent advances in high temperature electrolysis using solid oxide fuel cells: a review. J. Power Source. 203, 4–16.
Laguna-Bercero, M.A., Kilner, J.A., Skinner, S.J., 2010. Performance and characterization of (La, Sr) MnO3/YSZ and La0. 6Sr0. 4Co0. 2Fe0. 8O3 electrodes for solid oxide electrolysis cells. Chem. Mater. 22 (3), 1134–1141.
Langemann, M., et al., 2015. Validation and characterization of suitable materials for bipolar plates in PEM water electrolysis. Int. J. Hydrogen Energy 40 (35), 11385–11391.
Lee, H., et al., 2020. Economic and environmental analysis for PEM water electrolysis based on replacement moment and renewable electricity resources. Energy Convers. Manage. 224, 113477.
Lee, J., et al., 2021. High-efficiency anion-exchange membrane water electrolyzer enabled by ternary layered double hydroxide anode. Small 17 (28), 2100639.
Lee, T., 1971. Hydrogen over potential on pure metals in alkaline solution. J. Electrochem. Soc. 118 (8), 1278.
Lemus, R.G., Duart, J.M., 2010b. Updated hydrogen production costs and parities for conventional and renewable technologies. Int. J. Hydrogen Energy 35 (9).
Lemus, R.G., Duart, J.M.M., 2010a. Updated hydrogen production costs and parities for conventional and renewable technologies. Int. J. Hydrogen Energy 35 (9), 3929–3936.
Leng, Y., et al., 2012. Solid-state water electrolysis with an alkaline membrane. J. Am. Chem. Soc. 134 (22), 9054–9057.
Léon, A., et al., 2021. Effect of scaling-up on the performance and degradation of long-term operated electrolyte supported solid oxide cell, stack and module in electrolysis mode. J. Power Source. 510, 230346.
Lettenmeier, P., Gago, A.S., Friedrich, K.A., 2017. Protective coatings for low-cost bipolar plates and current collectors of proton exchange membrane electrolyzers for large scale energy storage from renewables. New Technologies in Protective Coatings. IntechOpen.
Li, D., et al., 2020. Highly quaternized polystyrene ionomers for high performance anion exchange membrane water electrolysers. Nat. Energy 5 (5), 378–385.
Li, J., Cai, Q., Amini Horri, B., 2023. Synthesis and densification of Mo/Mg co-doped apatite-type lanthanum silicate electrolyte with enhanced ionic conductivity. Chem.–A Eur. J. 29 (25), e202300021.
Li, Y., et al., 2013. Composite cathode based on Ni-loaded $La_{0.75}Sr_{0.25}Cr_{0.5}Mn_{0.5}O_{3-\delta}$ for direct steam electrolysis in an oxide-ion-conducting solid oxide electrolyzer. Int. J. Hydrogen Energy 38 (25), 10196–10207.

Li, Z., et al., 2015. Preparing alkaline anion exchange membrane with enhanced hydroxide conductivity via blending imidazolium-functionalized and sulfonated poly (ether ether ketone). J. Power Source. 288, 384–392.
Lim, A., et al., 2019. A study on electrode fabrication and operation variables affecting the performance of anion exchange membrane water electrolysis. J. Ind. Eng. Chem. 76, 410–418.
Ling, W., et al., 2019. Development strategy of hydrogen infrastructure industry in China. Strateg. Study of Chin. Acad. Eng. 21 (3), 76–83.
Ling, Y., et al., 2022. Stable solid oxide electrolysis cells with SSF-based symmetrical electrode for direct high-temperature steam electrolysis. Ceram. Int. 48 (1), 981–991.
Liu, C., 2021. Noble Metal Coated Porous Transport Layers for Polymer Electrolyte Membrane Water Electrolysis. RWTH Aachen University.
Liu, G., et al., 2014. A novel catalyst coated membrane embedded with Cs-substituted phosphotungstates for proton exchange membrane water electrolysis. Int. J. Hydrogen Energy 39 (27), 14531–14539.
Liu, Q., et al., 2010. Perovskite Sr2Fe1.5Mo0.5O6−δ as electrode materials for symmetrical solid oxide electrolysis cells. Int. J. Hydrogen Energy 35 (19), 10039–10044.
Liu, Z., et al., 2017. The effect of membrane on an alkaline water electrolyzer. Int. J. Hydrogen Energy 42 (50), 29661–29665.
López-Fernández, E., et al., 2022. Ionomer-Free Nickel-Iron bimetallic electrodes for efficient anion exchange membrane water electrolysis. Chem. Eng. J. 433, 133774.
Ma, H., et al., 2006. Study of ruthenium oxide catalyst for electrocatalytic performance in oxygen evolution. J. Mol. Catal. A Chem. 247 (1–2), 7–13.
Mahato, N., et al., 2015. Progress in material selection for solid oxide fuel cell technology: a review. Prog. Mater Sci. 72, 141–337.
Mališ, J., et al., 2016. Nafion 117 stability under conditions of PEM water electrolysis at elevated temperature and pressure. Int. J. Hydrogen Energy 41 (4), 2177–2188.
Manabe, A., et al., 2013. Basic study of alkaline water electrolysis. Electrochim. Acta 100, 249–256.
Mandin, P., et al., 2014. Bubble over-potential during two-phase alkaline water electrolysis. Electrochim. Acta 128, 248–258.
Marčeta Kaninski, M.P., et al., 2013. Cobalt-chrome activation of the nickel electrodes for the HER in alkaline water electrolysis – Part II. Int. J. Hydrogen Energy 38 (4), 1758–1764.
Marron, D.B., Toder, E.J., Austin, L., June 25, 2015. Taxing Carbon: what, Why, and How. Why, and How, p. 2015.
Marshall, A., et al., 2006. Electrochemical characterisation of IrxSn1-xO 2 powders as oxygen evolution electrocatalysts. Electrochim. Acta 51 (15), 3161–3167.
Marshall, A., et al., 2007. Hydrogen production by advanced proton exchange membrane (PEM) water electrolysersReduced energy consumption by improved electrocatalysis. Energy 32 (4), 431–436.
Maskalick, N., 1986. High temperature electrolysis cell performance characterization. Int. J. Hydrogen Energy 11 (9), 563–570.
Maslovara, S.L., et al., 2013. Novel ternary Ni–Co–Mo based ionic activator for efficient alkaline water electrolysis. Int. J. Hydrogen Energy 38 (36), 15928–15933.
Mayousse, E., et al., 2011. Synthesis and characterization of electrocatalysts for the oxygen evolution in PEM water electrolysis. Int. J. Hydrogen Energy 36 (17), 10474–10481.
McDowall, W., Eames, M., 2006. Forecasts, scenarios, visions, backcasts and roadmaps to the hydrogen economy: a review of the hydrogen futures literature. Energy Policy 34 (11), 1236–1250.
Medhoui, T., et al., 2006. Biomimetic approaches for the development of non-noble metal electrocatalysts. Application to PEM water electrolysis. In: Proceeds. 16th World Hydrogen Energy Conference (WHEC), Lyon, France. Citeseer.
Mehrpooya, M., Habibi, R., 2020. A review on hydrogen production thermochemical water-splitting cycles. J. Clean. Prod., 123836
Melaina, M., Bush, B., Penev, M., 2015. Overview of the Hydrogen Financial Analysis Scenario Tool (H2FAST); NREL (National Renewable Energy Laboratory). National Renewable Energy Lab.(NREL), Golden, COUnited States.
Menegaki, A., 2008. Valuation for renewable energy: a comparative review. Renew. Sustainab. Energy Rev. 12 (9), 2422–2437.
Milani, D., Kiani, A., McNaughton, R., 2020. Renewable-powered hydrogen economy from Australia's perspective. Int. J. Hydrogen Energy.
Miles, M., Huang, Y., Srinivasan, S., 1978. The oxygen electrode reaction in alkaline solutions on oxide electrodes prepared by the thermal decomposition method. J. Electrochem. Soc. 125 (12), 1931.
Miller, E.L., et al., 2020b. US Department of Energy hydrogen and fuel cell technologies perspectives. MRS Bull. 45 (1), 57–64.
Miller, H.A., et al., 2020a. Green hydrogen from anion exchange membrane water electrolysis: a review of recent developments in critical materials and operating conditions. Sustainab. Energy Fuel. 4 (5), 2114–2133.
Millet, P., et al., 2009. GenHyPEM: a research program on PEM water electrolysis supported by the European Commission. Int. J. Hydrogen Energy 34 (11), 4974–4982.
Millet, P., et al., 2010. PEM water electrolyzers: from electrocatalysis to stack development. Int. J. Hydrogen Energy 35 (10), 5043–5052.
Millet, P., et al., 2011. Electrochemical performances of PEM water electrolysis cells and perspectives. Int. J. Hydrogen Energy 36 (6), 4134–4142.
Millet, P., et al., 2012. Cell failure mechanisms in PEM water electrolyzers. Int. J. Hydrogen Energy 37 (22), 17478–17487.
Millet, P., Andolfatto, F., Durand, R., 1996. Design and performance of a solid polymer electrolyte water electrolyzer. Int. J. Hydrogen Energy 21 (2), 87–93.
Moçoteguy, P., Brisse, A., 2013. A review and comprehensive analysis of degradation mechanisms of solid oxide electrolysis cells. Int. J. Hydrogen Energy 38 (36), 15887–15902.
Mohammadzadeh, A., et al., 2020. *Mechanical Engineering of Solid Oxide Fuel Cell systems: Geometric design, Mechanical configuration, and Thermal analysis*, in *Design and Operation of Solid Oxide Fuel Cells*. Elsevier, pp. 85–130.
Motealleh, B., et al., 2021. Next-generation anion exchange membrane water electrolyzers operating for commercially relevant lifetimes. Int. J. Hydrogen Energy 46 (5), 3379–3386.
Mougin, J., et al., 2012. High temperature steam electrolysis stack with enhanced performance and durability. Energy Procedia 29, 445–454.
Mueller-Langer, F., et al., 2007. Techno-economic assessment of hydrogen production processes for the hydrogen economy for the short and medium term. Int. J. Hydrogen Energy 32 (16), 3797–3810.
Muradov, N., 2017. Low to near-zero CO2 production of hydrogen from fossil fuels: status and perspectives. Int. J. Hydrogen Energy 42 (20), 14058–14088.
Muradov, N., Veziroğlu, T., 2005. From hydrocarbon to hydrogen–carbon to hydrogen economy. Int. J. Hydrogen Energy 30 (3), 225–237.
Nakken, T., et al. *The Utsira wind-hydrogen system–operational experience*. in *European wind energy conference*. 2006.
Naughton, M.S., Brushett, F.R., Kenis, P.J., 2011. Carbonate resilience of flowing electrolyte-based alkaline fuel cells. J. Power Source. 196 (4), 1762–1768.
Navasa, M., Yuan, J., Sundén, B., 2015. Computational fluid dynamics approach for performance evaluation of a solid oxide electrolysis cell for hydrogen production. Appl. Energy 137, 867–876.
Nechache, A., Cassir, M., Ringuedé, A., 2014. Solid oxide electrolysis cell analysis by means of electrochemical impedance spectroscopy: a review. J. Power Source. 258, 164–181.
Newborough, M., Cooley, G., 2020. Developments in the global hydrogen market: the spectrum of hydrogen colours. Fuel Cells Bull. 2020 (11), 16–22.
Newell, R.G., Raimi, D., 2020. Global Energy Outlook Comparison methods: 2020 Update. Resources for the Future.
Ni, M., Leung, M.K., Leung, D.Y., 2008. Technological development of hydrogen production by solid oxide electrolyzer cell (SOEC). Int. J. Hydrogen Energy 33 (9), 2337–2354.
O'Brien, J.E., et al., 2007. Performance of planar high-temperature electrolysis stacks for hydrogen production from nuclear energy. Nucl. Technol. 158 (2), 118–131.
Oh, H.S., et al., 2016. Electrochemical catalyst–support effects and their stabilizing role for IrO x nanoparticle catalysts during the oxygen evolution reaction. J. Am. Chem. Soc. 138 (38), 12552–12563.
Olateju, B., Kumar, A., Secanell, M., 2016. A techno-economic assessment of large scale wind-hydrogen production with energy storage in Western Canada. Int. J. Hydrogen Energy 41 (21), 8755–8776.
Olateju, B., Monds, J., Kumar, A., 2014. Large scale hydrogen production from wind energy for the upgrading of bitumen from oil sands. Appl. Energy 118, 48–56.
Onda, K., et al., 2002. Performance analysis of polymer-electrolyte water electrolysis cell at a small-unit test cell and performance prediction of large stacked cell. J. Electrochem. Soc. 149 (8), A1069.
Oruc, O., Dincer, I., 2021. Assessing the potential of thermochemical water splitting cycles: a bridge towards for clean and sustainable hydrogen generation. Fuel 286, 119325.
Ozbilen, A., Dincer, I., Rosen, M.A., 2013. Comparative environmental impact and efficiency assessment of selected hydrogen production methods. Environ. Impact Assess. Rev. 42, 1–9.
Ozcan, H., El-Emam, R.S., Horri, B.A., 2022. Thermochemical looping technologies for clean hydrogen production–Current status and recent advances. J. Clean. Prod., 135295
Paciok, P., et al., 2015. Sensivity Analysis of a PEM Electrolyser Cathode with Respect to the Platinum and Nafion Loading. In: ECS Meeting Abstracts. IOP Publishing.
Padilha, J.C., et al., 2009. An evaluation of the potential of the use of wasted hydroelectric capacity to produce hydrogen to be used in fuel cells in order to decrease CO2 emissions in Brazil. Int. J. Hydrogen Energy 34 (19), 7898–7902.
Pandiyan, A., et al., 2019. Review of solid oxide electrolysis cells: a clean energy strategy for hydrogen generation. Nanomater. Energy 8 (1), 2–22.
Pantani, O., et al. *Electroactivity of Cobalt complexes for the reduction of protons into di-hydrogen. Application to PEM water electrolysis*. in *Proceeds. 16th World Hydrogen Energy Conference (WHEC), Lyon, France*. 2006.
Park, J.E., et al., 2019. High-performance anion-exchange membrane water electrolysis. Electrochim. Acta 295, 99–106.
Park, J.E., et al., 2022. Effect of catalyst layer designs for high-performance and durable anion-exchange membrane water electrolysis. J. Ind. Eng. Chem. 109, 453–460.
Parrado, C., et al., 2016. 2050 LCOE (Levelized Cost of Energy) projection for a hybrid PV (photovoltaic)-CSP (concentrated solar power) plant in the Atacama Desert, Chile. Energy 94, 422–430.
Parrondo, J., et al., 2014. Degradation of anion exchange membranes used for hydrogen production by ultrapure water electrolysis. RSC Adv. 4 (19), 9875–9879.
Pavel, C.C., et al., 2014. Highly efficient platinum group metal free based membrane-electrode assembly for anion exchange membrane water electrolysis. Angew. Chem. Int. Ed. 53 (5), 1378–1381.
Peters, D., et al., 2020. Gas Decarbonisation Pathways 2020–2050: gas for Climate.
Phillips, J., Fischer, L., 2021. Between Hope and Hype: a Hydrogen Vision for the UK.
Phillips, R., et al., 2017. Minimising the ohmic resistance of an alkaline electrolysis cell through effective cell design. Int. J. Hydrogen Energy 42 (38), 23986–23994.
Pivovar, B., 2017. H2@ Scale Workshop Report. National Renewable Energy Lab.(NREL), Golden, COUnited States.

Polonský, J., et al., 2014. Performance of a PEM water electrolyser using a TaC-supported iridium oxide electrocatalyst. Int. J. Hydrogen Energy 39 (7), 3072–3078.
Prasopchokkul, P., Seeharaj, P., Kim-Lohsoontorn, P., 2021. Ba0·5Sr0·5(Co0·8Fe0.2)1-xTaxO3-δ perovskite anode in solid oxide electrolysis cell for hydrogen production from high-temperature steam electrolysis. Int. J. Hydrogen Energy 46 (10), 7023–7036.
Qi, W., et al., 2014. Reversibly in-situ anchoring copper nanocatalyst in perovskite titanate cathode for direct high-temperature steam electrolysis. Int. J. Hydrogen Energy 39 (11), 5485–5496.
Quandt, K., Streicher, R., 1986. Concept and design of a 3.5 MW pilot plant for high temperature electrolysis of water vapor. Int. J. Hydrogen Energy 11 (5), 309–315.
Rafferty, K., 1999. Scaling in Geothermal Heat Pump Systems.
Raj, I.A., 1993. Nickel-based, binary-composite electrocatalysts for the cathodes in the energy-efficient industrial production of hydrogen from alkaline-water electrolytic cells. J. Mater. Sci. 28 (16), 4375–4382.
Ran, J., et al., 2014. Simultaneous enhancements of conductivity and stability for anion exchange membranes (AEMs) through precise structure design. Sci. Rep. 4 (1), 1–5.
Rasten, E., Hagen, G., Tunold, R., 2003. Electrocatalysis in water electrolysis with solid polymer electrolyte. Electrocatalysis: From Theory to Industrial Applications, September 22, 2002 - September 24, 2002. Elsevier Ltd, Como, Italy.
Ren, X., et al., 2014. Highly conductive anion exchange membrane for high power density fuel-cell performance. ACS Appl. Mater. Interfaces 6 (16), 13330–13333.
Roeb, M., et al., 2012. Materials-related aspects of thermochemical water and carbon dioxide splitting: a review. Materials (Basel) 5 (11), 2015–2054.
Roy, A., Watson, S., Infield, D., 2006. Comparison of electrical energy efficiency of atmospheric and high-pressure electrolysers. Int. J. Hydrogen Energy 31 (14), 1964–1979.
Rozain, C., Millet, P., 2014. Electrochemical characterization of polymer electrolyte membrane water electrolysis cells. Electrochim. Acta 131, 160–167.
Russell, J., Nuttall, L., Fickett, A., 1973. Hydrogen generation by solid polymer electrolyte water electrolysis. Am. Chem. Soc. Div. Fuel Chem. Prepr 18, 24–40.
Ruth, M.F., et al., 2020. The Technical and Economic Potential of the H2@ Scale Hydrogen Concept within the United States. National Renewable Energy Lab. (NREL), Golden, COUnited States.
Safari, F., Dincer, I., 2020. A review and comparative evaluation of thermochemical water splitting cycles for hydrogen production. Energy Convers. Manage. 205, 112182.
Santos, A.L., Cebola, M.J., Santos, D.M., 2021. Towards the hydrogen economy—a review of the parameters that influence the efficiency of alkaline water electrolyzers. Energies 14 (11), 3193.
Sapountzi, F.M., et al., 2017. Electrocatalysts for the generation of hydrogen, oxygen and synthesis gas. Prog. Energy Combust. Sci. 58, 1–35.
Saur, G., Ramsden, T., 2011. Wind Electrolysis: Hydrogen Cost Optimization.
Saveleva, V.A., et al., 2020. Insight into the mechanisms of high activity and stability of iridium supported on antimony-doped tin oxide aerogel for anodes of proton exchange membrane water electrolyzers. ACS Catal. 10 (4), 2508–2516.
Savoini, B., et al., 1998. Thermochemical reduction of yttria-stabilized-zirconia crystals: optical and electron microscopy. Phys. Rev. B 57 (21), 13439.
Schalenbach, M., et al., 2013. Pressurized PEM water electrolysis: efficiency and gas crossover. Int. J. Hydrogen Energy 38 (35), 14921–14933.
Schalenbach, M., et al., 2016. Acidic or alkaline? Towards a new perspective on the efficiency of water electrolysis. J. Electrochem. Soc. 163 (11), F3197.
Schalenbach, M., et al., 2018. The electrochemical dissolution of noble metals in alkaline media. Electrocatalysis 9 (2), 153–161.
Schefold, J., et al., 2020. 80,000 current on/off cycles in a one year long steam electrolysis test with a solid oxide cell. Int. J. Hydrogen Energy 45 (8), 5143–5154.
Schefold, J., Brisse, A., Poepke, H., 2017. 23,000 h steam electrolysis with an electrolyte supported solid oxide cell. Int. J. Hydrogen Energy 42 (19), 13415–13426.
Schefold, J., Brisse, A., Tietz, F., 2011. Nine thousand hours of operation of a solid oxide cell in steam electrolysis mode. J. Electrochem. Soc. 159 (2), A137.
Schüttauf, J.W., et al., 2016. Solar-to-hydrogen production at 14.2 % efficiency with silicon photovoltaics and earth-abundant electrocatalysts. J. Electrochem. Soc. 163 (10), F1177.
Sedlak, J.M., Lawrance, R.J., Enos, J.F., 1981. Advances in oxygen evolution catalysis in solid polymer electrolyte water electrolysis. Int. J. Hydrogen Energy 6 (2), 159–165.
Serna, Á., Tadeo, F., 2014. Offshore hydrogen production from wave energy. Int. J. Hydrogen Energy 39 (3), 1549–1557.
Shaikh, S.P., Muchtar, A., Somalu, M.R., 2015. A review on the selection of anode materials for solid-oxide fuel cells. Renew. Sustainab. Energy Rev. 51, 1–8.
Shaner, M.R., et al., 2016. A comparative technoeconomic analysis of renewable hydrogen production using solar energy. Energy Environ. Sci. 9 (7), 2354–2371.
Shidong, S., et al., 2007. An improved catalyst-coated membrane structure for PEM water electrolyzer. Electrochem. Solid State Lett. 10 (8), 122–125.
Shidong, S., et al., 2008. Electrochemical investigation of electrocatalysts for the oxygen evolution reaction in PEM water electrolyzers. Int. J. Hydrogen Energy 33 (19), 4955–4961.
Shiva Kumar, S., et al., 2018. Synthesis of titanium (IV) oxide composite membrane for hydrogen production through alkaline water electrolysis. S. Afr. J. Chem. Eng. 25, 54–61.
Shiva Kumar, S., Himabindu, V., 2020. Boron-Doped Carbon nanoparticles supported palladium as an efficient hydrogen evolution electrode in PEM water electrolysis. Renew. Energy 146, 2281–2290.
Silander, D., 2020. The EU and Agenda 2050: new political entrepreneurship in its making. Implementing Sustainable Development Goals in Europe. Edward Elgar Publishing.
Singh, R., et al., 2007. Novel electrocatalysts for generating oxygen from alkaline water electrolysis. Electrochem. Commun. 9 (6), 1369–1373.
Siracusano, S., et al., 2012. An electrochemical study of a PEM stack for water electrolysis. Int. J. Hydrogen Energy 37 (2), 1939–1946.
Siracusano, S., et al., 2014. Performance analysis of short-side-chain Aquivion® perfluorosulfonic acid polymer for proton exchange membrane water electrolysis. J. Memb. Sci. 466, 1–7.
Siracusano, S., et al., 2015. Performance of a PEM water electrolyser combining an IrRu-oxide anode electrocatalyst and a short-side chain Aquivion membrane. Int. J. Hydrogen Energy 40 (42), 14430–14435.
Siracusano, S., et al., 2017. The influence of iridium chemical oxidation state on the performance and durability of oxygen evolution catalysts in PEM electrolysis. J. Power Sources 366, 105–114.
Siracusano, S., et al., 2018b. Degradation issues of PEM electrolysis MEAs. Renew. Energy. 123, 52–57.
Siracusano, S., et al., 2018a. Degradation issues of PEM electrolysis MEAs. Renew. Energy 123, 52–57.
Sivanantham, A., Shanmugam, S., 2017. Nickel selenide supported on nickel foam as an efficient and durable non-precious electrocatalyst for the alkaline water electrolysis. Appl. Catal. B 203, 485–493.
Skulimowska, A., et al., 2014. Proton exchange membrane water electrolysis with short-side-chain Aquivion® membrane and IrO2 anode catalyst. Int. J. Hydrogen Energy 39 (12), 6307–6316.
Slade, S., et al., 2002. Ionic conductivity of an extruded Nafion 1100 EW series of membranes. J. Electrochem. Soc. 149 (12), A1556.
Slavcheva, E., et al., 2007. Sputtered iridium oxide films as electrocatalysts for water splitting via PEM electrolysis. Electrochim. Acta 52 (12), 3889–3894.
Slavcheva, E., et al., 2015. Ebonex supported iridium as anode catalyst for PEM water electrolysis. Int. J. Hydrogen Energy 40 (35), 11356–11361.
Solmaz, R., et al., 2016. Enhancement of electrochemical activity of Raney-type NiZn coatings by modifying with PtRu binary deposits: application for alkaline water electrolysis. Int. J. Hydrogen Energy 41 (3), 1432–1440.
Steinfeld, A., 2005. Solar thermochemical production of hydrogen—a review. Sol. Energy 78 (5), 603–615.
Stiller, C., et al., 2005. Finite-volume modeling and hybrid-cycle performance of planar and tubular solid oxide fuel cells. J. Power Source. 141 (2), 227–240.
Stojmenović, M., Dodevski, V., 2021. 16 Ceramic electrolytes for solid oxide fuel cells (SOFCs) as alternative energy sources. Adv. Ceram. Applic. 205.
Sun, S., et al., 2014. Investigations on degradation of the long-term proton exchange membrane water electrolysis stack. J. Power Source. 267, 515–520.
Taibi, E., Miranda, R., Carmo, M., 2020. Green Hydrogen Cost Reduction.
Tajuddin, A.A.H., et al., 2021. Corrosion-resistant non-noble metal electrodes for PEM-type water electrolyzer. Int. J. Hydrogen Energy 46 (78), 38603–38611.
Takenaka, H., et al., 1982. Solid polymer electrolyte water electrolysis. Int. J. Hydrogen Energy 7 (5), 397–403.
Tang, E., et al., 2018. Solid Oxide Based Electrolysis and Stack Technology With Ultra-High Electrolysis Current Density (>3A/cm2) and Efficiency. FuelCell Energy, Inc., Danbury, CTUnited States.
Tang, H., et al., 2007. A degradation study of Nafion proton exchange membrane of PEM fuel cells. J. Power Source. 170 (1), 85–92.
Tawfik, H., Hung, Y., Mahajan, D., 2007. Metal bipolar plates for PEM fuel cell—A review. J. Power Source. 163 (2), 755–767.
Temeev, A.A., Belokopytov, V.P., Temeev, S.A., 2006. An integrated system of the floating wave energy converter and electrolytic hydrogen producer. Renew. Energy 31 (2), 225–239.
Terezo, A.J., et al., 2001. Separation of transport, charge storage and reaction processes of porous electrocatalytic IrO2 and IrO2/Nb2O5 electrodes. J. Electroanal. Chem. 508 (1–2), 59–69.
Thangavel, P., et al., 2020. Graphene-nanoplatelets-supported NiFe-MOF: high-efficiency and ultra-stable oxygen electrodes for sustained alkaline anion exchange membrane water electrolysis. Energy Environ. Sci. 13 (10), 3447–3458.
Thomsen, E.C., et al., 2009. Performance of lanthanum strontium manganite electrodes at high pressure. J. Power Source. 191 (2), 217–224.
Tietz, F., et al., 2013. Degradation phenomena in a solid oxide electrolysis cell after 9000 h of operation. J. Power Source. 223, 129–135.
Tiwari, P., et al., 2019. A new class of bubble-free water electrolyzer that is intrinsically highly efficient. Int. J. Hydrogen Energy 44 (42), 23568–23579.
Tonekabonimoghaddam, M., Shamiri, A., 2021. Simulation and sensitivity analysis for various geometries and optimization of solid oxide fuel cells: a review. Eng 2 (3), 386–415.
Torrell, M., et al., 2015. Co-electrolysis of steam and CO2 in full-ceramic symmetrical SOECs: a strategy for avoiding the use of hydrogen as a safe gas. Faraday Discuss. 182 (0), 241–255.
Tsekouras, G., Irvine, J.T.S., 2011. The role of defect chemistry in strontium titanates utilised for high temperature steam electrolysis. J. Mater. Chem. 21 (25), 9367–9376.
Tsekouras, G., Neagu, D., Irvine, J.T.S., 2013. Step-change in high temperature steam electrolysis performance of perovskite oxide cathodes with exsolution of B-site dopants. Energy Environ. Sci. 6 (1), 256–266.
Tunold, R., et al., 2010. Materials for electrocatalysis of oxygen evolution process in PEM water electrolysis cells. ECS Trans. 25 (23), 103.
van Renssen, S., 2020. The hydrogen solution? Nat. Clim. Chang. 10 (9), 799–801.
Verheul, B., 2019. Overview of Hydrogen and Fuel Cell Developments in China. Holland Innovation Network China.
Vincent, I., Bessarabov, D., 2018. Low cost hydrogen production by anion exchange membrane electrolysis: a review. Renew. Sustainab. Energy Rev. 81, 1690–1704.

Vincent, I., Kruger, A., Bessarabov, D., 2017. Development of efficient membrane electrode assembly for low cost hydrogen production by anion exchange membrane electrolysis. Int. J. Hydrogen Energy 42 (16), 10752–10761.
Wan, L., et al., 2021. H2SO4-doped polybenzimidazole membranes for hydrogen production with acid-alkaline amphoteric water electrolysis. J. Memb. Sci. 618, 118642.
Wan, L., et al., 2022. Dual regulation both intrinsic activity and mass transport for self-supported electrodes using in anion exchange membrane water electrolysis. Chem. Eng. J. 431, 133942.
Wang, H., et al., 2018. Novel composite electrolytes of Zr0. 92Y0. 08O2-α (8YSZ)-low melting point glass powder for intermediate temperature solid oxide fuel cells. Mater. (Basel) 11 (7), 1221.
Wang, J., et al., 2021. Kinetics of oxygen reaction in porous La0. 6Sr0. 4Co0. 2Fe0. 8O3–δ-Ce0. 8Gd0. 2O1. 9 composite electrodes for solid oxide cells. Int. J. Hydrogen Energy.
Wang, Y., et al., 2016. Syngas production on a symmetrical solid oxide H2O/CO2 co-electrolysis cell with Sr2Fe1.5Mo0.5O6–Sm0.2Ce0.8O1.9 electrodes. J. Power Source. 305, 240–248.
Wang, Y., et al., 2020. Degradation of solid oxide electrolysis cells: phenomena, mechanisms, and emerging mitigation strategies—a review. J. Mater. Sci. Technol. 55, 35–55.
Wang, Z., Mori, M., Araki, T., 2010. Steam electrolysis performance of intermediate-temperature solid oxide electrolysis cell and efficiency of hydrogen production system at 300 Nm3 h− 1. Int. J. Hydrogen Energy 35 (10), 4451–4458.
Warde, C., et al. *Status and Programs at Westinghouse*. in *Program and Abstracts*, ERDA/EPRI Fuel Cell Seminar, Palo Alto, CA (June 1976). 1976.
Wei, G., et al., 2010. The stability of MEA in SPE water electrolysis for hydrogen production. Int. J. Hydrogen Energy 35 (9), 3951–3957.
Wendt, H., Hofmann, H., Plzak, V., 1989. Materials research and development of electrocatalysts for alkaline water electrolysis. Mater. Chem. Phys. 22 (1–2), 27–49.
Williams, K., 2007. The g4-econs economic evaluation tool for generation iv reactor systems. Transact.-Am. Nucl. Soc. 96, 131.
Wongsuwan, W., et al., 2001. A review of chemical heat pump technology and applications. Appl. Therm. Eng. 21 (15), 1489–1519.
Wu, L., et al., 2014. The stability of hydrogen evolution activity and corrosion behavior of porous Ni3Al–Mo electrode in alkaline solution during long-term electrolysis. Energy 67, 19–26.
Wu, X., Scott, K., 2012. A polymethacrylate-based quaternary ammonium OH− ionomer binder for non-precious metal alkaline anion exchange membrane water electrolysers. J. Power Source. 214, 124–129.
Xiao, L., et al., 2012. First implementation of alkaline polymer electrolyte water electrolysis working only with pure water. Energy Environ. Sci. 5 (7), 7869–7871.
Xu, S., et al., 2013. Composite cathode based on Fe-loaded LSCM for steam electrolysis in an oxide-ion-conducting solid oxide electrolyser. J. Power Source. 239, 332–340.
Xu, S., et al., 2014. Perovskite chromates cathode with resolved and anchored nickel nano-particles for direct high-temperature steam electrolysis. J. Power Source. 246, 346–355.
Yang, K., Lee, K., Lee, T., 2008. Preliminary Cost Estimates for Nuclear Hydrogen Production. HTSE System.
Yang, Z., Zhang, G., Lin, B., 2015. Performance evaluation and optimum analysis of a photovoltaic-driven electrolyzer system for hydrogen production. Int. J. Hydrogen Energy 40 (8), 3170–3179.
Yu, B., et al., 2008. Advance in highly efficient hydrogen production by high temperature steam electrolysis. Sci. China Ser. B: Chem. 51 (4), 289–304.
Yu, H., Yi, B., 2018. Hydrogen for energy storage and hydrogen production from electrolysis. Strateg. Study Chin. Acad. Eng. 20 (3), 58–65.
Yu, M., Wang, K., Vredenburg, H., 2021. Insights into low-carbon hydrogen production methods: green, blue and aqua hydrogen. Int. J. Hydrogen Energy 46 (41), 21261–21273.
Zahid, M., Schefold, J., Brisse, A., 2010. High-temperature water electrolysis using planar solid oxide fuel cell technology: a review. Hydrogen and Fuel Cells, Fundamentals, Technologies and Applications. Wiley-VCH, Weinheim, pp. 227–242.
Zeng, K., Zhang, D., 2010. Recent progress in alkaline water electrolysis for hydrogen production and applications. Prog. Energy Combust. Sci. 36 (3), 307–326.
Zeng, L., Zhao, T., 2015a. Integrated inorganic membrane electrode assembly with layered double hydroxides as ionic conductors for anion exchange membrane water electrolysis. Nano Energy 11, 110–118.
Zeng, L., Zhao, T.S., 2015b. Integrated inorganic membrane electrode assembly with layered double hydroxides as ionic conductors for anion exchange membrane water electrolysis. Nano Energy 11, 110–118.
Zhang, D., Zeng, K., 2012. Evaluating the behavior of electrolytic gas bubbles and their effect on the cell voltage in alkaline water electrolysis. Ind. Eng. Chem. Res. 51 (42), 13825–13832.
Zhang, J., et al., 2011. Electrochemical Technologies for Energy Storage and Conversion, 2 Volume Set, 1. John Wiley & Sons.
Zhang, J., et al., 2014. *Composite titanate cathode enhanced with* in situ *grown nickel nanocatalyst for direct steam electrolysis*. New J. Chem. 38 (8), 3434–3442.
Zhang, L., et al., 2017. High activity oxide $Pr_{0.3}Sr_{0.7}Ti_{0.3}Fe_{0.7}O_{3-\delta}$ as cathode of SOEC for direct high-temperature steam electrolysis. Int. J. Hydrogen Energy 42 (17), 12104–12110.
Zhang, X., et al., 2013. Improved durability of SOEC stacks for high temperature electrolysis. Int. J. Hydrogen Energy 38 (1), 20–28.
Zhang, X., et al., 2015. Experimental design, operation, and results of a 4 kW high temperature steam electrolysis experiment. J. Power Source. 297, 90–97.
Zhao, T., et al., 2022. Heterostructured V-doped $Ni_2P/Ni_{12}P_5$ electrocatalysts for hydrogen evolution in anion exchange membrane water electrolyzers. Small 18 (40), 2204758.
Zheng, Y., et al., 2017. A review of high temperature co-electrolysis of H_2O and CO_2 to produce sustainable fuels using solid oxide electrolysis cells (SOECs): advanced materials and technology. Chem. Soc. Rev. 46 (5), 1427–1463.
Ziems, C., Tannert, D., Krautz, H.J., 2012. Project presentation: Design and Installation of Advanced High Pressure Alkaline Electrolyzer-Prototypes, 29. Energy Procedia, pp. 744–753.
Zohuri, B., 2019. Large-scale hydrogen production. Hydrogen Energy. Springer, pp. 229–255.
Zongqiang, M., et al., 2007. Study on a novel manufacturing process of membrane electrode assemblies for solid polymer electrolyte water electrolysis. Electrochem. Commun. 9 (4), 667–670.
Zoulias, E., et al., 2004. A review on water electrolysis. Tcjst 4 (2), 41–71.